To the Graduate Council:

I am submitting herewith a thesis written by Don Randall Womack entitled "Electrochemical Behavior of Rhodium(I) Alkylisocyanides In Various Solvents and Supporting Electrolyte Systems." I have examined the final copy of this thesis for form and content and recommend that it be accepted in partial fulfillment of the requirements for the degree of Master of Science, with a major in Chemistry.

Clifton Woods

Clifton Woods, Major Professor

We have read this thesis
and recommend its acceptance:

William E Bull

James Q. Chambers

Accepted for the Council:

L Evans Roth

Vice Chancellor
Graduate Studies and Research

ELECTROCHEMICAL BEHAVIOR OF RHODIUM(I) ALKYLISOCYANIDES IN VARIOUS SOLVENTS AND SUPPORTING ELECTROLYTE SYSTEMS

A Thesis

Presented for the

Master of Science

Degree

The University of Tennessee, Knoxville

Don Randall Womack

December 1981

3055511

DEDICATION

To Edwina and Teri.

ACKNOWLEDGEMENTS

I would like to express my appreciation to The University of Tennessee, Knoxville for financial aid in the form of a teaching assistantship.

Thanks must first go to Dr. Clifton Woods, III for his guidance, support, and patience throughout my stay here at UT-K. Also I would like to thank Rob Peterson, Billy Anderson, Dr. J. Q. Chambers, Paul Enlow, Peter Tinsley, and Celeste Daffron for giving me invaluable aid in my research.

Special thanks to my Mom and Bug for helping me through many financial binds and to Cindy, Sonya, Edwina, Gary, Granny and the rest of my family for their support.

The following people have given me pleasant memories of Tennessee: Richard Hutchings, Vince Conrad, J. D. Vargo, Dr. Woods, Peter and Wendy Tinsley, Celeste Daffron, Dave Abbott, Dr. William Bull, Paul Enlow, and the rest of the gang.

Finally, a very special thanks to Gayle Fritts, for not only typing this thesis, but for being a friend.

ABSTRACT

The electrochemical behavior of several rhodium(I) dimers containing two bridging diphenylphosphinomethane ligands and alkyl isocyanide ligands have been examined using cyclic voltammetry, coulometry and bulk electrolysis. The effect of coordinating and non-coordinating solvents and supporting electrolytes on the oxidation of these complexes has been investigated. A correlation of the ease of oxidation and the bulkiness of the isocyanide ligand has been observed.

Several new rhodium(II) dimers have been prepared by oxidation of the rhodium(I) dimers in acetonitrile or in methylene chloride. These novel complexes have been characterized using infrared spectroscopy and elemental analysis.

TABLE OF CONTENTS

CHAPTER		PAGE
I.	INTRODUCTION	1
	A. Literature Review	1
	B. Statement of the Problem	7
II.	EXPERIMENTAL	9
	A. Chemicals	9
	B. Cyclic Voltammetry	14
	C. Coulometry	16
	D. Spectroscopy	17
	E. Elemental Analysis	18
	F. Synthesis of Dimeric Rhodium(I) and Rhodium(II) Species	18
III.	RESULTS AND DISCUSSION	23
	A. Methylene Chloride	23
	B. Acetonitrile	57
	C. Nitromethane	62
	D. Summary	64
LIST OF REFERENCES		67
VITA		69

LIST OF TABLES

TABLE PAGE

I. CYCLIC VOLTAMMETRIC PEAK POTENTIALS OF $[Rh_2(RNC)_4(dpm)_2][PF_6]_2$ COMPLEXES IN THE CH_2Cl_2/TBAH SYSTEM 26

II. CYCLIC VOLTAMMETRIC PARAMETERS OF THE Ox1/R1 COUPLE OF THE $[Rh_2(RNC)_4(dpm)_2][PF_6]_2$ COMPLEXES IN THE CH_2Cl/TBAH SYSTEM 27

III. CYCLIC VOLTAMMETRIC PEAK POTENTIALS OF $[Rh_2(RNC)_4(dpm)_2][PF_6]_2$ COMPLEXES IN THE CH_2Cl_2/TBAB SYSTEM 34

IV. HALF-WAVE POTENTIALS FOR $[Rh_2(RNC)_4(dpm)_2][PF_6]_2$ COMPLEXES IN THE CH_2Cl_2/TBAP SYSTEM 49

V. VOLTAMMETRIC PEAK POTENTIALS FOR $[Rh_2(RNC)_4(dpm)_2][PF_6]_2$ COMPLEXES IN THE CH_2Cl_2/TBAN SYSTEM 54

VI. VOLTAMMETRIC PEAK POTENTIALS FOR COMPLEXES $[Rh_2(RNC)_4(dpm)_2][PF_6]_2$ COMPLEXES IN THE CH_3CN/TBAH SYSTEM 59

LIST OF FIGURES

FIGURE		PAGE
1.	Molecular orbital diagram of a rhodium(I) dimer	4
2.	Low temperature electrochemical cell	15
3.	Cyclic voltammograms of $[(\underline{n}\text{-}C_4H_9NC)_4Rh_2(dpm)_2][PF_6]_2$ in the CH_2Cl_2/TBAH system	24
4.	Plots of current versus the square root of sweep rate for $[Rh_2(RNC)_4(dpm)_2][PF_6]_2$ complexes: A. R = $\underline{n}\text{-}C_4H_9$; B. R = $\underline{i}\text{-}C_3H_7$; C. R = $\underline{s}\text{-}C_4H_9$; D. R = C_6H_{11}; E. R = $\underline{t}\text{-}C_4H_9$	28
5.	Cyclic voltammogram of $[(\underline{n}\text{-}C_4H_9NC)_4Rh_2(dpm)_2][PF_6]_2$ after oxidation at +0.85 volts in the CH_2Cl_2/TBAH system	29
6.	Cyclic voltammogram of $[(\underline{n}\text{-}C_4H_9NC)_4Rh_2(dpm)_2][PF_6]_2$ in the CH_2Cl_2/TBAB system	31
7.	Cyclic voltammogram of $[(\underline{t}\text{-}C_4H_9NC)_4Rh_2(dpm)_2][PF_6]_2$ in the CH_2Cl_2/TBAB system	33
8.	Cyclic voltammogram of $[(\underline{n}\text{-}C_4H_9NC)_4Rh_2(dpm)_2][PF_6]_2$ after oxidation at +0.88 volts in the CH_2Cl_2/TBAB system	35
9.	Cyclic voltammogram of $[(\underline{n}\text{-}C_4H_9NC)_4Rh_2(dpm)_2][PF_6]_2$ after oxidation at +1.35 volts in the CH_2Cl_2/TBAB system	36
10.	Cyclic voltammogram of $[(\underline{n}\text{-}C_4H_9NC)_4Rh_2(dpm)_2][PF_6]_2$ after reduction at -1.00 volts of the oxidized solution at +1.35 volts in the CH_2Cl_2/TBAB system	37
11.	Cyclic voltammogram of $[(\underline{n}\text{-}C_4H_9NC)_4Rh_2(dpm)_2][PF_6]_2$ in the CH_2Cl_2/TBAP system	39
12.	Cyclic voltammogram of $[(\underline{i}\text{-}C_3H_7NC)_4Rh_2(dpm)_2][PF_6]_2$ in the CH_2Cl_2/TBAP system	40

FIGURE PAGE

13. Cyclic voltammogram of $[(\underline{s}\text{-}C_4H_9NC)_4Rh_2(dpm)_2][PF_6]_2$ in the CH_2Cl_2/TBAP system 41

14. Cyclic voltammogram of $[(C_6H_{11}NC)_4Rh_2(dpm)_2][PF_6]_2$ in the CH_2Cl_2/TBAP system 42

15. Cyclic voltammogram of $[(\underline{t}\text{-}C_4H_9NC)_4Rh_2(dpm)_2][PF_6]_2$ in the CH_2Cl_2/TBAP system 44

16. Low temperature cyclic voltammograms of $[(\underline{n}\text{-}C_4H_9NC)_4Rh_2(dpm)_2][PF_6]_2$ in the CH_2Cl_2/TBAP system 45

17. Possible rhodium mixed oxidation state tetrameric species . 47

18. Cyclic voltammogram of $[(\underline{n}\text{-}C_4H_9NC)_4Rh_2(dpm)_2][PF_6]_2$ after oxidation at +0.77 volts in the CH_2Cl_2/TBAP system 48

19. Cyclic voltammogram of $[(\underline{n}\text{-}C_4H_9NC)_4Rh_2(dpm)_2][PF_6]_2$ after oxidation at +1.30 volts in the CH_2Cl_2/TBAP system 51

20. Cyclic voltammogram of $[(\underline{n}\text{-}C_4H_9NC)_4Rh_2(dpm)_2][PF_6]_2$ after reduction at -1.00 volts of the oxidized solution at -1.30 volts 52

21. Cyclic voltammograms of (A) $[(\underline{n}\text{-}C_4H_9NC)_4Rh_2(dpm)_2][PF_6]_2$ and (B) $[(\underline{i}\text{-}C_3H_7NC)_4Rh_2(dpm)_2][PF_6]_2$ in the CH_2Cl_2/TBAN system 53

22. Cyclic voltammorgam of $[(\underline{n}\text{-}C_4H_9NC)_4Rh_2(dpm)_2][PF_6]_2$ after oxidation at +0.79 volts in the CH_2Cl_2/TBAN system 55

23. Cyclic voltammogram of $[(\underline{n}\text{-}C_4H_9NC)_4Rh_2(dpm)_2][PF_6]_2$ in the CH_3CN/TBAH system 58

24. Cyclic voltammogram of $[(\underline{i}\text{-}C_3H_7NC)_4Rh_2(dpm)_2[PF_6]_2$ after oxidation at +1.30 volts in the CH_3CN/TBAH system 61

FIGURE PAGE

25. Cyclic voltammogram of $[(\underline{i}\text{-}C_3H_7NC)_4Rh_2(dpm)_2][BF_4]_2$ after oxidation at +1.00 volts in the CH_3CN/TBAB system 63

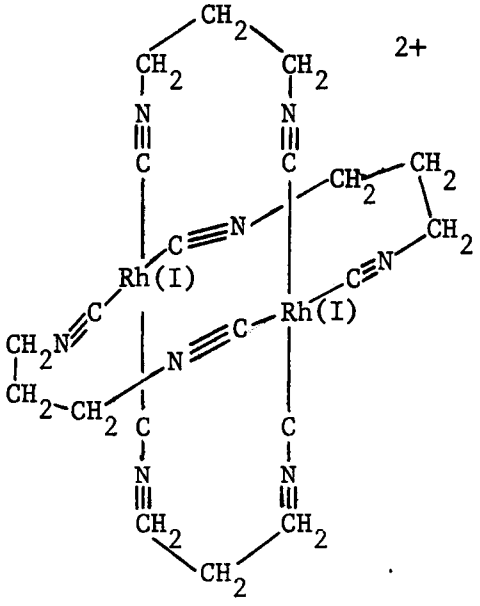
26. Cyclic voltammogram of $[(\underline{i}\text{-}C_3H_7NC)_4Rh_2(dpm)_2][PF_6]_2$ in the CH_3NO_2/TBAH system 65

CHAPTER I

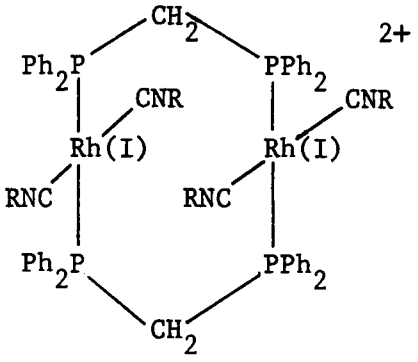
INTRODUCTION

A. Literature Review

Interest in dinuclear rhodium(I) isocyanide complexes has increased since 1976 when Gray and coworkers[1] synthesized complex 1, $[Rh_2(bridge)_4][BPh_4]_2$ (bridge = 1,3-diisocyanopropane), and Balch[2,3] synthesized structurally and electronically similar dimers containing the cations $[(Rh_2(RNC)_4(Ph_2PCH_2PPh_2)_2]^{2+}$, 2a-2e. These complexes can be isolated as the crystalline hexafluorophosphate, tetraphenylborate, or tetrafluoroborate salts.



1



2a: R = n-C_4H_9

2b: R = i-C_3H_7

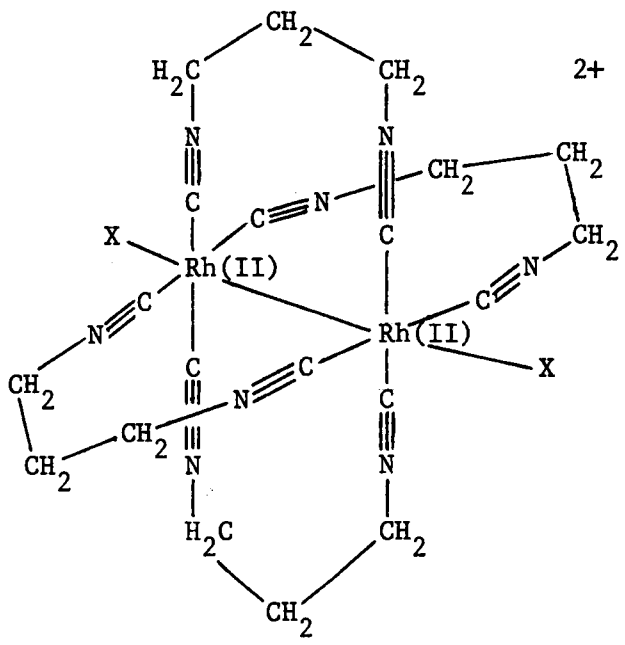
2c: R = C_6H_{11}

2d: R = s-C_4H_9

2e: R = t-C_4H_9

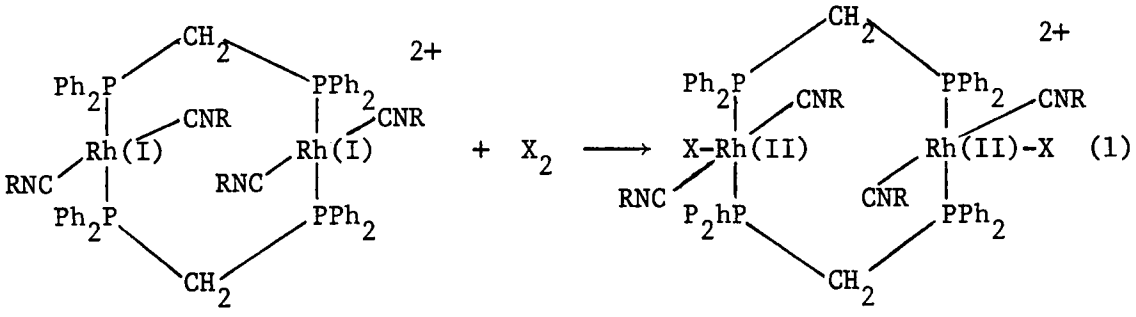
Complex 1 has been shown to form aggregates in solution as a result of metal-metal interactions between dimeric units. UV-visible spectroscopic data suggest that in concentrated solutions tetrameric and hexameric species can form. Complexes 2a-2e (page 1) however, have not been shown to form similar oligomeric units, presumably due to the steric requirements of the phenyl groups on the diphosphine ligand.

When substrates such as I_2 and Br_2 are added to dilute acetonitrile solutions of 1 (page 1), oxidative addition reactions occur to yield d^7 rhodium(II) dimers, 3, which contain a formal Rh-Rh bond.



3

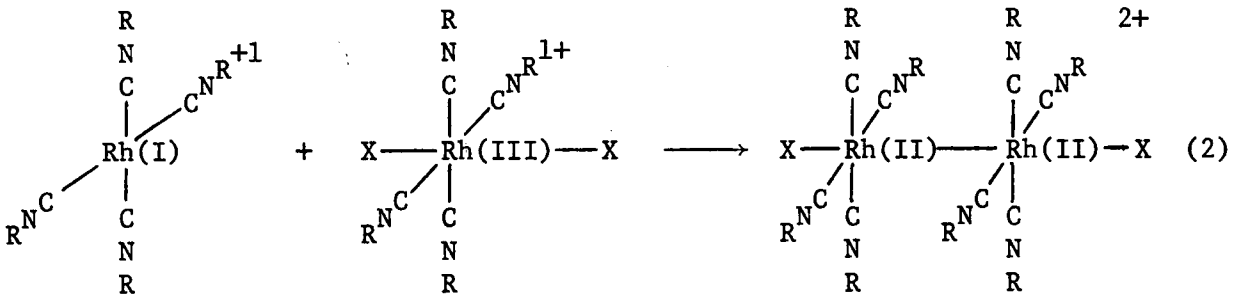
The analogous complexes 2a-2e (page 1) also undergo similar oxidative addition reactions with Br_2 and I_2 molecules (Equation 1).



(1)

X_2 = Br_2, I_2, CF_3SSCF_3, CH_2SSCH_3, $C_4H_9SSC_4H_9$

M. M. Olmstead and A. L. Balch[4] have shown that Rh(II)-Rh(II) dimers can also be formed when rhodium(I) complexes of the type, $Rh(CNR)_4^{1+}$, and rhodium(III) complexes of the type, $Rh(CNR)_4X_2^{1+}$ are mixed in solution. This reduction-oxidation process is accompanied by transfer of X from one rhodium to another with simultaneous formation of a Rh-Rh bond (Equation 2).



(2)

R = CH_3, n-C_4H_9, $C_6H_5CH_2$, C_6H_{11}

X = Br, I

The electronic nature of rhodium(I) dimers can be described by the modified molecular orbital (MO) diagram presented in Figure 1. When two monomeric units are brought face to face, the dz^2 (a_{1g}) orbitals interact to give a bonding and an antibonding MO. Likewise, interaction between the empty π^* orbitals (a_{2u}) leads to bonding and antibonding MO's. For rhodium(I) dimers, occupation of these orbitals leads

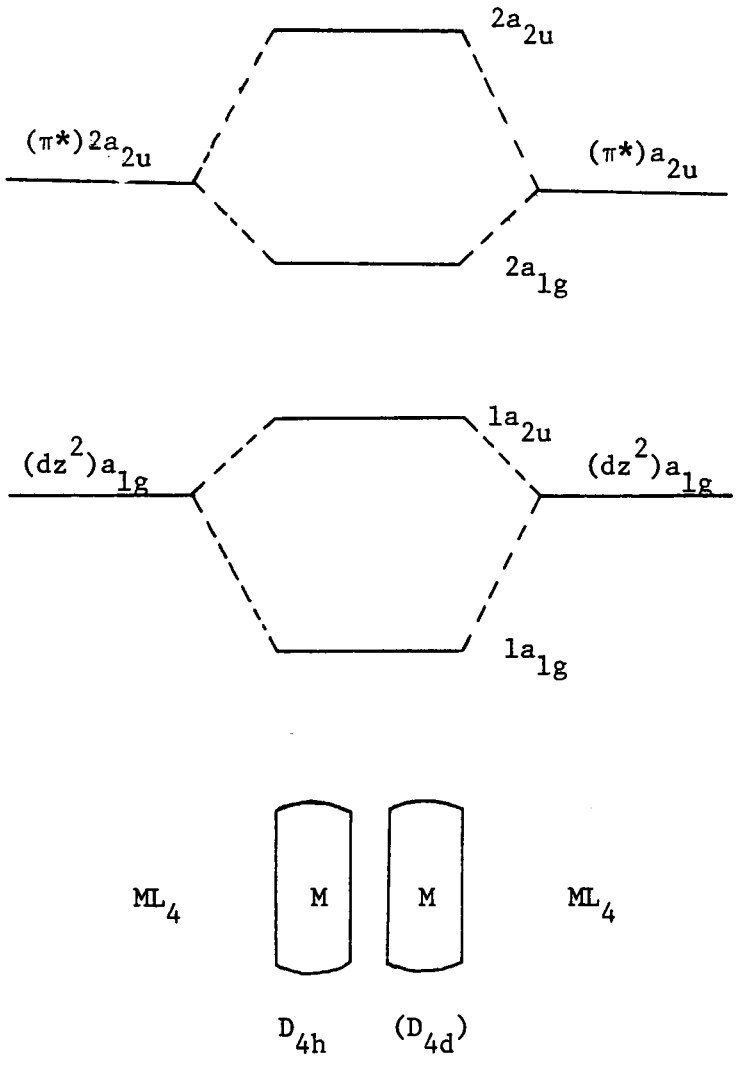


Figure 1. Molecular orbital diagram of rhodium(I) dimer.

to $1a_{2u}$ as the highest occupied molecular orbital (HOMO) and $2a_{1g}$ as the lowest unoccupied molecular orbital (LUMO).[2,5] Removal of two electrons from the $1a_{2u}$ orbital during oxidative addition leads to a formal Rh(II)-Rh(II) bond.

The rhodium(II) formulation is substantiated by the fact that the single isocyanide (CN) infrared (IR) stretching frequency shifts to a higher frequency upon formation of the rhodium(II) species. Donation of d-electrons to the π^* orbitals on the isocyanide lignads decreases as the metal oxidation state increases, thereby increasing the CN bond order and the IR stretching frequency.[3]

Added interest in complex 1 (page 1) results from its ability to generate hydrogen gas when acidic solutions of 1 are irradiated with visible radiation. When placed in aqueous 12M hydrochloric acid solution, the electronic absorption spectrum exhibits an intense band at 578 nm. Irradiation at 546 nm produces a yellow product and a gas. The yellow product has been identified as $[Rh_2(bridge)_4Cl_2]^{2+}$ and the gas as hydrogen. The originally proposed mechanism suggests that an intermediate in the hydrogen generation process is a Rh(1½)-Rh(1½) species produced by a one electron oxidation (Equation 3).[6]

$$[(Cl^-)Rh(I)\text{---}Rh(I)(H^+)]^{2+} \xrightarrow{546\ (nm)} [(Cl^-)\text{---}Rh(I\tfrac{1}{2})\text{---}Rh(1\tfrac{1}{2})\text{---}(H\cdot)]^{*2+}$$
$$[(Cl^-)\text{---}Rh(I\tfrac{1}{2})\text{---}Rh(I\tfrac{1}{2})\text{---}(H\cdot)]^{*2+} \xrightarrow[HCl]{Fast} [Cl\text{-}Rh(II)\text{-}Rh(II)\text{-}Cl]^{2+} + H_2 \qquad (3)$$

Later studies[7] have shown that this proposed mechanism is not entirely correct. The reaction actually occurs in two distinct steps. The first of which is a thermal reaction of complex 1 (page 1) with HCl to form H_2 and the tetramer, $[Rh_2(bridge)_4Cl]_2^{4+}$. The next step is a photochemical reaction (λ = 546 nm) of the tetramer with H^+ to form H_2

and $[Rh_2(bridge)_4Cl_2]^{2+}$, Equation 4.

$$[Rh_2(bridge)_4]^{2+} + HCl \longrightarrow \tfrac{1}{2}[Rh_2(bridge)_4Cl]_2^{4+} + \tfrac{1}{2}H_2$$
$$\tfrac{1}{2}[Rh_2(bridge)_4Cl]_2^{4+} + HCl \xrightarrow[546\ nm]{h\nu} [Rh_2(bridge)_4Cl_2]^{2+} + \tfrac{1}{2}H_2 \qquad (4)$$

The tetranuclear nature of the intermediate has been confirmed by crystal structure determination which indicates that the measured bond lengths (2.93 Å for outer Rh-Rh bonds and 2.78 Å for inner Rh-Rh bonds) are consistent with a Rh(I)-Rh(II)-Rh(II)-Rh(I) mixed oxidation state species instead of the Rh(1½)-Rh(1½) species proposed earlier.[8] Assignment of the redox state for $[Rh_2(bridge)_4Cl]_2^{4+}$ was based on reductive titration of $[Rh_2(bridge)_4Cl_2]^{2+}$ with chromium(II), Cr^{2+}, by spectroscopically measuring the loss of Cr^{2+} as it was converted to Cr^{3+} in aqueous 6M hydrochloric acid. When $[Rh_2(bridge)_4Cl_2]^{2+}$ was reduced by Cr^{2+} solutions the only reduction product found was $[Rh_2(bridge)_4Cl]_2^{4+}$. An experimental value of 1.0 ± 0.1 was obtained for the ratio $[Rh_2(bridge)_4Cl_2]^{2+}/Cr^{2+}$, with the reaction occuring according to equation 5.[8]

$$[Rh_2(bridge)_4Cl_2]^{2+} + Cr^{2+} \longrightarrow \tfrac{1}{2}[Rh_2(bridge)_4Cl]_2^{4+} + Cl^- + Cr^{3+} \qquad (5)$$

Even though rhodium(I) and rhodium(II) dimers seem to be readily susceptible to oxidation-reduction reactions, studies of their electrochemical behavior have only recently begun. K. R. Mann and B. A. Parkinson[9] investigated the behavior of $[Rh_2(bridge)_4]_2^{6+}$ at a rotating glassy carbon electrode. When $[Rh_2(bridge)_4]^{2+}$ is dissolved in concentrated sulfuric or methanesulfonic acid and diluted to 0.5 mM, air oxidation yields $[Rh_2(bridge)_4]_2^{6+}$ upon mixing.

This species exhibits an oxidation wave near the onset of the oxidation wave of water at +1.10 volts. Addition of small amounts of chloride ion shifts the oxidation wave to more negative potentials because of a stronger bonding of the chloride ion by the oxidized complex, $[Rh_2(bridge)_4]^{4+}$, than by the reduced complex, $[Rh_2(bridge)_4]_2^{6+}$. By monitoring the disappearance of known amounts of cerium(IV), the oxidation was found to involve two electrons per $[Rh_2(bridge)_4]_2^{6+}$. The overall chemical and electrochemical process for the oxidation reaction at the electrode in the presence of chloride ion is presented in Equation 6.

$$[Rh_2(bridge)_4]_2^{6+} + Cl^- \longrightarrow [Rh_4(bridge)_8Cl]^{5+} \quad 10$$
$$[Rh_4(bridge)_8Cl]^{5+} + 3Cl^- \longrightarrow 2[Rh_2(bridge)_4Cl_2]^{2+} + 2e^- \quad (6)$$

B. Statement of the Problem

The ease with which rhodium(I) isocyanide dimers tend to undergo oxidative-addition reactions, and the lack of electrochemical data on these complexes lead to the electrochemical investigation which is the subject of this thesis. One of the goals of this study is a better understanding of the electrochemical behavior of Rh(I) dimers.

Due to its ability to form tetramers in aqueous solutions, complex 1 (page 1) produces an intermediate with mixed oxidation states during the photochemical hydrogen generation reaction. However, complexes 2a-2e (page 1) will not likely form tetramers in solution during oxidation because of steric hindrance of the phenyl groups on the diphosphine ligand. Therefore, it is also of interest in this study to see if electrochemical techniques can be used to generate mixed oxidation state species for complexes 2a-2e (page 1).

Since there are no previously reported electrochemical studies of complexes 2a-2e (page 1), this investigation should demonstrate the differences in the electron transfer behavior of complex 1 (page 1) and complexes 2a-2e (page 1). Due to the tendency of the dimeric rhodium(I) complexes to undergo oxidative-addition, this research also deals with the effects that coordinating species have on the electrochemical behavior of rhodium(I) dimers.

CHAPTER II

EXPERIMENTAL

A. Chemicals

1. Reagents

a. Isopropylisocyanide, (i-C_3H_7NC), Aldrich. Reagent grade i-C_3H_7NC was used without further purification.

b. Normal Butylisocyanide, (n-C_4H_9NC), Aldrich. Reagent grade n-C_4H_9NC was used without further purification.

c. Tetrabutylisocyanide, (t-C_4H_9NC), Aldrich. Reagent grade t-C_4H_9NC was used without further purification.

d. Cyclohexylisocyanide, ($C_6H_{11}NC$), Aldrich. Reagent grade $C_6H_{11}NC$ was used without further purification.

e. Secondary Butylamine, Eastman. Reagent grade sec-butylamine was used without further purification.

f. Ethylformate, Eastman. Reagent grade ethylformate was used without further purification.

g. Para-Toluenesulfonic acid monohydrate, Fisher Scientific. Certified ACS p-toluenesulfonic acid monohydrate was used without further purification.

h. Para-toluenesulfonyl Chloride, Eastman. Reagent grade p-toluenesulfonyl chloride was used without further purification.

i. Quinoline, Eastman. Reagent grade quinoline was freshly distilled from zinc before use.

j. Secondary Butylformamide. Sec-butylformamide was prepared by the procedure of J. Casanova, N. D. Werner, and R. E. Schuster.[11] To a solution of 0.074 moles of sec-butylamine and 0.147 moles of

ethylformate, a trace of p-toluenesulfonic acid monohydrate was added. The mixture was refluxed for 16 hr. and the excess ethylformate and ethanol were removed by distillation. The formamide was then distilled at 0.5 mm mercury (Hg).

k. Secondary Butylisocyanide, (s-C_4H_9NC). Sec-butylformamide (0.25 moles) was added dropwise to a stirred solution of p-toluenesulfonyl chloride (0.38 moles) and quinoline (1.00 moles) at 70°C and 60 mm Hg. The volatile product was distilled into a receiver cooled in liquid nitrogen. The product was characterized by proton nuclear magnetic resonance spectroscopy (NMR). The NMR parameters compare favorably with values reported by Casanova, Werner, and Schurster.[11]

l. Rhodium(III) Trichloride Trihydrate, ($RhCl_3 \cdot 3H_2O$), Strem. Reagent grade $RhCl_3 \cdot 3H_2O$ was used without further purification.

m. Bis(diphenylphosphino)methane, (dpm), Strem. Reagent grade dpm was used without further purification.

n. Sodium Tetrafluoroborate, ($NaBF_4$), Fisher Scientific. Reagent grade $NaBF_4$ was used without further purification.

o. 1,5-Cyclooctadiene, Aldrich. Reagent grade 1,5-cycloctadiene was used without further purification.

p. Di-μ-Chloro-Bis(η4-1,5-Cyclooctadiene)Dirhodium(I), $[RhCl(C_8H_{10})]_2$. This compound was prepared from a modified version of the procedure presented by J. Chatt and L. M. Venanzi.[12] $RhCl_3 \cdot 3H_2O$ (1.20 g) was introduced into a 100-mL round bottom flask connected to a reflux condenser filled with a nitrogen atmosphere. Twelve mL of deoxygenated ethanol water (5:1) and 1.8 mL of 1,5-cyclooctadiene were then added to the flask. The mixture was stirred briskly and heated

at reflux under a nitrogen atmosphere for 18 hours. The product was filtered and washed with pentane. The product was then washed with methanol water (1:5) until the washings no longer contained chloride ions. The product was dried under vacuum. The yield was 98%.

q. Tetrabutylammonium Iodide, (TBAI), Aldrich. Reagent grade TBAI was used without further purification.

r. Tetrabutylammonium Hydroxide, (TBAOH), Aldrich. A 40% by weight aqueous solution of TBAOH was used as received.

s. Hydrogen Hexafluorophosphate, (HPF_6), Alfa. A 60% by volume aqueous solution of HPF_6 was used as received.

t. Nitric Acid, (HNO_3), Fisher Scientific. Certified ACS reagent grade HNO_3 was used without further purification.

u. Perchloric Acid, ($HClO_4$), Fisher Scientific. Reagent grade ACS 70% by volume $HClO_4$ was used without further purification.

v. Sodium Perchlorate, ($NaClO_4$), G. Fedrich Smith Chemical Company. Reagent grade $NaClO_4$ was used without further purification.

w. Calcium Chloride, ($CaCl_2$), Fisher Scientific. Reagent grade anhydrous $CaCl_2$ was used without further purification.

x. Magnesium Sulfate, ($MgSO_4$), Fisher Scientific. Reagent grade anhydrous $MgSO_4$ was used without further purification.

2. Solvents

a. Acetonitrile, (CH_3CN), Aldrich. Spectrophotometric grade CH_3CN was used as purchased.

b. Methylene Chloride, (CH_2Cl_2), Fisher Scientific. Certified ACS Spectroanalyzed CH_2Cl_2 was used as purchased.

c. Nitromethane, (CH_3NO_2), Fisher Scientific. Certified ACS CH_3NO_2 was purified by drying over $CaCl_2$ followed by distillation.[13]

d. Methanol, (CH_3OH), Fisher Scientific. Certified ACS CH_3OH was used without further purification.

e. Methylene Chloride, Fisher Scientific. Certified ACS methylene chloride was used without further purification.

f. Acetone, Fisher Scientific. Certified ACS acetone was used without further purification.

g. Normal Propanol, Mallinkrodt. Reagent grade n-propanol was used without further purification.

h. Diethyl Ether, (ether), Fisher Scientific. Certified ACS anhydrous ether was used without further purification.

i. Doubly-Distilled Water, (water, H_2O). Distilled water from the departmental still was redistilled using a WE-2 Continuous Still (Kontes Glass Company).

j. Absolute Elthanol, (ethanol), Aaper Alcohol. Certified ACS ethanol was used as purchased.

k. Normal Pentane, (pentane), Eastman. Reagent grade pentane was used as purchased.

l. Chloroform, Fisher Scientific. Certified ACS chloroform was used without further purification.

m. Ligroin, Fisher Scientific. Certified ACS 30-60 Ligroin was used as purchased.

3. Supporting Electrolytes

a. Tetrabutylammonium Hexafluorophosphate, (TBAH). Two procedures were used to prepare TBAH. Early preparations were by metathesis of TBAI with $NaPF_6$ in water. Later preparations involved neutralization of TBAOH with HPF_6. The products from both preparations were recrystallized three times from acteone-water. Before use, TBAH was dried for

3 hours under vacuum at 45°C.

b. Tetrabutylammonium Perchlorate, (TBAP). TBAP was prepared either by metathesis of TBAI with $NaClO_4$ or by neutralization of TBAOH with $HClO_4$. Purification was achieved by three recrystallizations from acetone-water followed by drying under vacuum for 3 hours at 45°C.

c. Tetrabutylammonium Tetrafluoroborate, (TBAB), Fisher. Reagent grade TBAB was purified by three recrystallizations from methanol-water followed by drying under vacuum for 6 hours at 45°C.

d. Tetrabutylammonium Nitrate, (TBAN). TBAN was prepared by exact neutralization of TBAOH with HNO_3. The solution was extracted with chloroform four times. After the chloroform layer was reduced in volume, ligroin was added to precipitate the TBAN. The product was purified by three recrystallizations from chloroform-ligroin and the solid was dried for 21 hours under vacuum at 50°C.

4. Miscellaneous

a. Argon, (Ar), Selox Inc. Prepurified Ar was used without further drying.

b. Nitrogen, (N_2), Selox Inc. Prepurfied N_2 was used as purchased, and in cases where dried N_2 was needed, the gas was passed through a column containing $MgSO_4$.

c. Sodium Metal (Na), Fisher Scientific. Reagent grade sodium metal was used as purchased.

d. Nujol, Plough, Inc. Nujol was used after drying over metallic sodium.

e. Potassium Bromide, (KBr), Fisher Scientific. Certified ACS KBr was used after drying for 3 hours at 80°C.

B. Cyclic Voltammetry

1. Electrodes

A conventional three electrode system was employed for all voltammetry. The reference electrode was a standard saturated calomel electrode (SCE) which was always separated from the bulk solution by a fine frit. The working electrode was a 0.24 cm^2 platinum button electrode (Beckman) and the counter electrode was a 2.76 cm^2 platinum grid.

2. Electrochemical Cell

The cell used for voltammetry was a one compartment cell fitted with a porous bottom and an inlet glass tube to allow the solution to be degassed and blanketed with Ar. All measurements using this cell were performed at room temperature.

For low temperature studies, a one compartment cell of the design used by R. P. Van Duyne and C. N. Reilley[14] was employed, Figure 2. The reference, working, and auxiliary electrodes were placed in close proximity to minimize the uncompensated ohmic drop. The cell was made variable in temperature by using coiled copper tubing immersed in liquid nitrogen with dry N_2 gas passing through the coils into the jacket surrounding the cell's inner compartment. The solvent was degassed with Ar and a blanket of Ar was maintained over the solution during the experiment.

Low temperatures were measured using a Fluke 2100A Digital Thermometer equipped with an iron-constantan thermocouple. The thermocouple was placed directly in the solution under investigation.

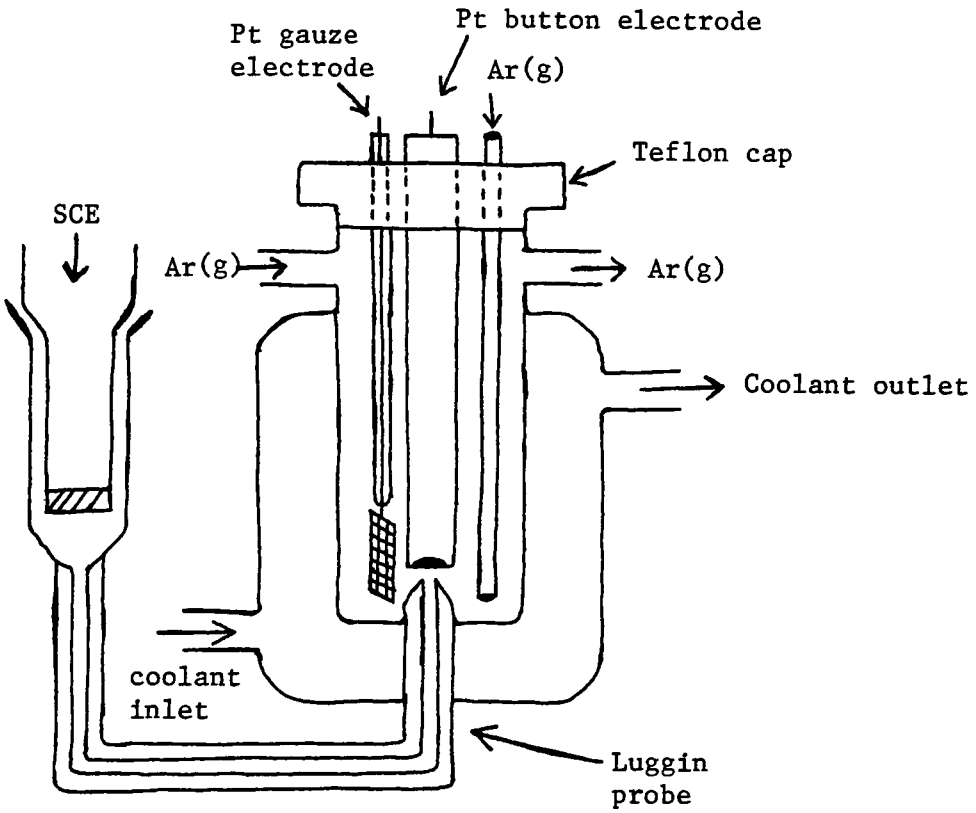


Figure 2. Low temperature electrochemical cell.

3. Instrumentation

a. Potentiostat. All voltammetry was performed using a PAR 364 Polarographic Analyzer.

b. Sine Wave Generator. The potentiostat was used in conjunction with a sine wave generator designed by Woodward and coworkers[15] and constructed by The University of Tennessee Chemistry Department Electronic Shop.

c. Recorder. Experimental curves were recorded on a Houston Instruments 2000 Omnigraphic X-Y Recorder.

4. Solvents and Supporting Electrolytes

Spectroanalyzed CH_2Cl_2 was used with 0.1M TBAH, TBAB, TBAP, or TBAN. When CH_3CN was used as the solvent, TBAH or TBAB were used as the supporting electrolytes. CH_3NO_2 was used with TBAH as the supporting electrolyte.

C. Coulometry

1. Electrodes

A three electrode system was employed in which the isolated counter electrode was a carbon rod; the working electrode was a 25 cm^2 platinum grid; and the reference electrode was a SCE of standard design. A fine glass frit always separated the SCE from the bulk solution.

2. Electrochemical Cell

A three compartment cell was used for all coulometry. The working electrode compartment was fitted with a fine frit bottom which was used for degassing with Ar and for stirring the solution during the experiment. The counter electrode compartment was separated from the

working compartment by a central compartment fitted on each side by fine frits.

3. Coulometer

All coulometric experiments were performed with a PAR 173 Potentiostat/Galvanostat which was equipped with a PAR 179 Digital Coulometer.

4. Solvents and Supporting Electrolytes

All systems used for coulometry were similar to those used in voltammetry where the concentration of the supporting electrolyte was always 0.1 Molar.

D. Spectroscopy

1. Proton Nuclear Magnetic Resonance Spectroscopy

All samples analyzed by proton NMR were neat liquids containing tetramethylsilane (TMS) as the internal standard. A Varian T-60A NMR Spectrometer was used for all measurements.

2. Infrared Spectroscopy

Infrared spectra were obtained using a Digital FTS-20 C/V Fourier Transform Infrared Spectrometer. All samples were examined in the solid either as a Nujol mull between thin polyethylene sheets or as KBr pellets. The mulls were sealed between the polyethylene sheets using a Clamco Super Sealer.

3. Ultraviolet-Visible Spectroscopy

A Cary 17 Spectrophotometer was used to obtain all ultraviolet-visible (UV-Vis) spectra. Quartz cells (Fisher Scientific) of

1.0 cm pathlength were used to obtain all UV-Vis spectra. CH_3CN and CH_2Cl_2, both of which were of spectroscopic grade, were used to make solutions of known concentrations. Spectra were recorded using the solvent in the reference beam.

E. Elemental Analysis

Galbraith Laboratories, Inc. of Knoxville, Tennessee performed all elemental analysis.

F. Synthesis of Dimeric Rhodium(I) and Rhodium(II) Species

All alkyl isocyanide rhodium(I) complexes of the type 2a-2e (page 1) were synthesized using the procedure outlined by A. L. Balch, J. W. Habadie, and G. Delker.[3]

1. Rhodium(2+), tetrakis(2-isocyanopropane)bis[μ-methylenebis[diphenylphosphine-P:P´]]bis[hexafluorophosphate(1-)], $[(i\text{-}C_3H_7NC)_4Rh_2(dppm)_2][PF_6]_2$, 2b (page 1).

To a stirred yellow solution of 1.00 g (2.00 mmole) of $[(1,5\text{-}C_8H_{10})RhCl]_2$ and 1.54 g (4.00 mmol) of dpm in 75-mL of methanol, 0.55 g (8.0 mmol) of $i\text{-}C_3H_7NC$ was added dropwise. The solvents had previously been deoxygenated using N_2 and the reaction was carried out under an atmosphere of N_2. The violet solution was stirred for approximately 40 minutes then filtered to remove any unreacted material. A solution of 0.65 g (4.00 mmol) of NH_4PF_6 in 25-mL of methanol was added to the filtrate.

This solution was again stirred briskly for 30 minutes to allow complete crystallization to occur. The violet precipitate was collected by filtration and purified by recrystallization from methylene chloride/methanol or acetone/1-propanol. The yield was 40%.

The IR spectrum of a Nujol mull shows ν_{CN} at 2145 cm^{-1}(s) and 2166(sh). The UV-Vis spectrum in CH_2Cl_2 shows peaks at 545 nm and 319 nm. The UV-Vis spectrum in CH_3CN shows peaks at 554 nm, 374 nm, and 318 nm.

2. Rhodium(2+), tetrakis(2-isocyanopropane)bis[μ-methylenebis[diphenylphosphine-P:P′]]bis[tetrafluoroborate(1-)], $[(i\text{-}C_3H_7NC)_4Rh_2(dpm)_2][BF_4]_2$, 4.

The procedure was similar to that used to prepare complex 2b (page 1). The yield was 34% and the UV-Vis spectrum obtained in CH_3CN shows peaks at 553 nm, 371 nm, and 317.2 nm.

3. Rhodium(2+), tetrakis(1-isocyanobutane)bis[μ-methylenebis[diphenylphosphine-P:P′]]bis[hexafluorophosphate(1-)], $[(n\text{-}C_4H_9NC)_4Rh_2(dpm)_2][PF_6]_2$, 2a (page 1).

The procedure was similar to that used to prepare complex 2b (page 1). The yield was 30%. The IR spectrum of a Nujol mull shows ν_{CN} at 2160(s) cm^{-1} and 2183(sh) cm^{-1} (lit.[2] (solid): 2165 cm^{-1} and 2146 cm^{-1}). The UV-Vis spectrum obtained in CH_2Cl_2 shows bands at 546 nm and 318 nm and the spectrum obtained in CH_3CN shows peaks at 558 nm, 385 nm, and 313 nm (lit.[2] for BPh_4^- salt in CH_3CN: 560 nm, 338 nm (sh), and 320 nm).

4. Rhodium(2+), tetrakis(2-isocyanobutane)bis[μ-methylenebis[diphenylphosphine-P:P′]]bis[hexafluorophosphate(1-)], $[(s\text{-}C_4H_9NC)_4Rh_2(dpm)_2][PF_6]^2$, 2c (page 1).

The procedure was similar to that used to prepare complex 2b (page 1). The yield was 60%. The IR spectrum of a Nujol mull shows ν_{CN}

at 2138 cm^{-1}(s) and 2162 cm^{-1}(w). The UV-Vis spectrum obtained in CH_2Cl_2 shows peaks at 548 nm, 393 nm, and 318 nm.

5. Rhodium(2+), tetrakis(2-isocyano-2-methylpropane)bis[μ-methylenebis[diphenylphosphine-P:P´]]bis[hexafluorophosphate(1-)], $[t\text{-}C_4H_9CN)_4Rh_2(dpm)_2][PF_6]_2$, 2e (page 1).

The procedure was similar to that used to prepare complex 2b (page 1). The yield was 60%. The IR spectrum of a Nujol mull shows ν_{CN} at 2125 cm^{-1}(s) and 2168 cm^{-1}(w) (lit.[2] (solid): 2122 cm^{-1} and 2152 cm^{-1}). The UV-Vis spectrum obtained in CH_2Cl_2 shows peaks at 520 nm, 345 nm(sh) and 321 nm. The UV-Vis spectrum obtained in CH_3CN shows peaks at 521 nm, 380 nm, and 318 nm (lit.[2]: 523 nm, 337 nm, and 320 nm).

6. Rhodium(2+), tetrakis(isocyanocyclohexane)bis[μ-methylenebis[diphenylphosphine-P:P´]]bis[hexafluorophosphate(1-)], $[C_6H_{11}NC)_4Rh_2(dpm)_2][PF_6]_2$, 2d (page 1).

The procedure was similar to that used to prepare complex 2b (page 1). The yield was 50%. The IR spectrum of a Nujol mull shows ν_{CN} at 2140 cm^{-1}(s) and 2168 cm^{-1}(w) (lit.[2] (solid) for BPh_4^- salt: 2136 cm^{-1} and 2157 cm^{-1}). The UV-Vis spectrum obtained in CH_2Cl_2 shows peaks at 538 nm, 337 nm, and 320 nm. The UV-Vis spectrum obtained in CH_3CN shows peaks at 545 nm, 387 nm, and 318 nm (lit.[2] for BPh_4^- salt: 550 nm, 337 nm, and 320 nm).

7. Rhodium(3+), tetrakis(1-isocyanobutane)-μ-nitratobis[μ-methylenebis[diphenylphosphine-P:P´]]tris[hexafluorophosphate(1-)], $[(n\text{-}C_4H_9NC)_4Rh_2(NO_3)(dpm)_2][PF_6]_3$, 5.

A violet solution of 100 mg of complex 2a (page 1) in 40 mL of CH_2Cl_2 containing 0.1M TBAN was oxidized at a potential of +0.79 volts

while being stirred with Ar. The charge recorded indicated a loss of two electrons (n = 1.95) per dimer. The light brown electrolysis product was separated from the supporting electrolyte by extracting the electrolysis solution with water. The TBAN dissolved in the water layer and the electrolysis product remained in the CH_2Cl_2. The CH_2Cl_2 layer was then stripped to dryness on a rotary-evaporator and the residue was dried under vacuum at room temperature. The product was dissolved in methanol and a four fold excess of KPF_6 was added to ensure that the counter ion was PF_6^-. Enough water was added to give a 4:1 methanol/water mixture which was then extracted with CH_2Cl_2. The CH_2Cl_2 layer was removed then reduced in volume after which ether was added to precipitate the product. Recrystallization was achieved by dissolving the product in CH_2Cl_2 and adding ether to the cloud point and cooling at -10°C for 6 hours. The brown product was filtered and dried under vacuum for 12 hours. The yield was 41%.

The IR spectrum (KBr disk; cm^{-1}): 3160(w), 2965(s), 2938(m), 2875(m), 2214(s)(ν_{CN}), 2221(s)(ν_{CN}), 1650(w), 1620(w), 1590(w), 1575(w), 1510(w), 1486(m), 1468(m), 1448(s), 1150(w), 1122(w), 1098(m), 1000(w), 839 (ν_{PF_6})(vs), 781(m), 742(s), 695(m), 558(ν_{PF_6})(vs), 520(m), 508(w), 485(w). Anal. Calcd for $C_{70}H_{80}F_{18}N_5O_3P_7Rh_2$: C, 46.61; H, 4.47; N, 3.88. Found: C, 46.79; H, 4.80; N, 3.90.

8. Rhodium(4+), tetrakis(2-isocyanopropane)bis[μ-methylenebis[diphenylphosphine-P:P']]tetrakis[tetrafluoroborate(1-)]Hemiacetonitrile adduct $[(i\text{-}C_3H_7NC)_4Rh_2(dpm)_2][BF_4]_4 \cdot \frac{1}{2}CH_3CN$, 6.

A deep violet solution of 100 mg of complex 4 (page 19) in 40 mL of CH_3CN containing 0.1M TBAB was oxidized at +1.00 volts while being stirred with Ar. The charge consumed indicated an electron loss of

approximately two (n = 1.86). The yellow solution was evaporated. The dried residue was placed in water and stirred for 4 hours to dissolve the supporting electrolyte. To ensure complete removal of TBAB, the product was stirred with water and filtered three additional times. After the final filtration the product was washed with ether. Recrystallization was achieved by dissolving the product in CH_2Cl_2/CH_3CN (1:1), followed by the addition of ether until the cloud point was reached. The mixture was cooled for 6 hours at -10°C. After filtration the product was wahsed with ether. The yield was 67%.

The IR spectrum (KBr disk, cm^{-1}): 3400(m,b), 3050(m) 2985(m), 2960(m), 2930(m), 2872(m), 2227(s)(ν_{CN}), 1670(w), 1620(w), 1570(w), 1525(m), 1460(m), 1440(s), 1370(w), 1330(m), 1290(w), 1090(s), 1035(s), 780(m), 730(s) 690(s), 520(s), 485(m), 430(w). Anal. Calcd for $C_{67}H_{73.5}B_4F_{16}N_{4.5}P_4Rh_2$: C, 49.71; H, 4.58; N, 3.89. Found: C, 50.10; H, 5.29; N, 3.91.

CHAPTER III

RESULTS AND DISCUSSION

Various solvents and supporting electrolytes were used to examine the electrochemical behavior of complexes 2a-2e (page 1). Each complex used for cyclic voltammetry and controlled potential coulometry studies contained the hexafluorophosphate anion as the counter ion unless otherwise stated. Supporting electrolyte concentrations were 0.1M and complex concentrations were 1×10^{-3}M. The sweep rate for cyclic voltammetry was generally 100 mV/sec unless otherwise stated.

The major concern of this thesis is the elucidaton of oxidation processes of the complexes 2a-2e (page 1) under different supporting electrolyte and solvent conditions. Each of the complexes exhibits a reduction wave at approximately -1.40 volts and oxidation waves resulting from this reduction at approximately -0.40 volts and -0.15 volts. The reduction wave at -1.40 volts and corresponding oxidation waves were not examined as a part of the work presented in this thesis.

A. Methylene Chloride

1. Tetrabutylammonium Hexafluorophosphate

In order to compare the electrochemical behavior of complexes 2a-2e (page 1) under conditions of a noncoordinating solvent and supporting electrolyte, the CH_2Cl_2/TBAH system was used. Cyclic voltammograms for each complex were similar to that shown in Figure 3A for complex 2a (page 1).

The oxidation wave at +1.30 volts (0x2) gives rise to a series of reduction waves at -5.30 volts, -0.67 volts, and -0.95 volts. Due

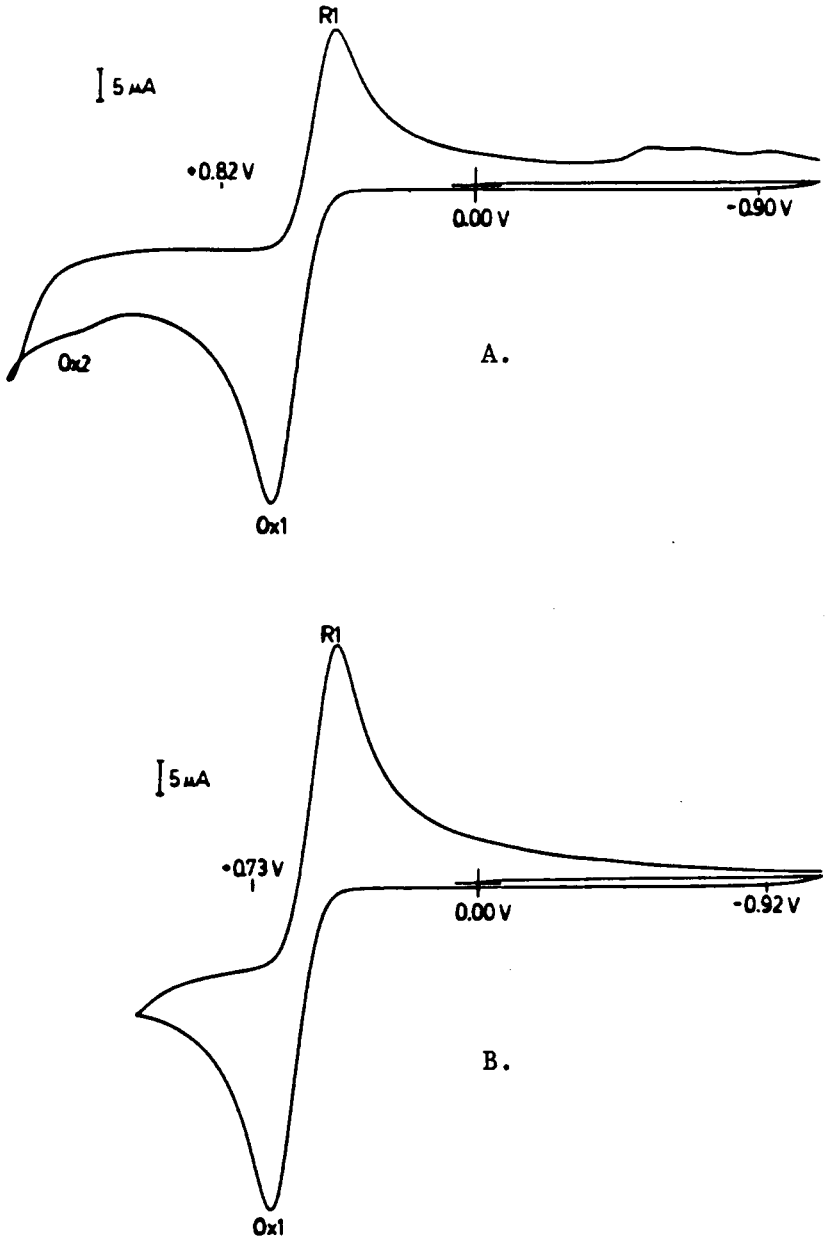


Figure 3. Cyclic voltammograms of $[(\underline{n}\text{-}C_4H_9NC)_4Rh_2(dpm)_2][PF_6]_2$ in the CH_2Cl_2/TBAH system.

Conditions A and B: Conc. 3×10^{-3}M; 0.1M TBAH; sweep rate 100 mV sec^{-1}; SCE.

to the proximity of Ox2 to the solvent limit the processes giving rise to this wave could not be investigated using coulometry and electrolysis. The principal oxidation wave, Ox1, which occurs at a potential of +0.65 volts, is coupled only to the reduction wave, R1, at +0.47 volts, Figure 3B. The cyclic voltammetric data for complexes 2a-2e (page 1) are presented in Table I.

The quasi-reversibility of the couple Ox1/R1 is shown by the fact that (1) the peak potentials are sweep rate dependent, and (2) the difference in peak potentials is greater than 58 mV and increases with an increase in sweep rate. The current ratios (i_{pa}/i_{pc}) are generally greater than one, and plots of peak current versus the square root of the sweep rate deviate slightly from linearity between sweep rates of 20 mV/sec and 200 mV/sec[16] (Table II and Figure 4.)

Controlled potential coulometry performed on complex 2a (page 1) at +0.85 volts suggests an electron count of one (n = 1.09). Cyclic voltammagrams of the oxidized solution show an increase in the peak currents of R2, R3, and R4 and substantial reduction in the peak current of R1, Figure 5A and 5B. The residual R1 peak current could mean that the electrolysis was incomplete or that some of the oxidation product remains intact. The virtual absence of R1 during sweeps in a negative direction from +0.85 volts indicates that the oxidation product either breaks down or reacts, on the coulometric time scale, with the solvent and/or supporting electrolyte to form more stable products. The products, however, could not be isolated and characterized. The reappearance of Ox1 after sweeping through R2, R3, and R4 indicates that the dimer remains intact after oxidation

TABLE I

CYCLIC VOLTAMMETRIC PEAK POTENTIALS[a]

OF $[Rh_2(RNC)_4(dpm)_2][PF_6]_2$ COMPLEXES

IN THE CH_2Cl_2/TBAH SYSTEM

R	Ox1	Ox2	R1	R2	R3	R4	R5
n-C_4H_9	0.65	1.30	0.47	b	-0.53	-0.67	-0.95
i-C_3H_7	0.71	1.38	0.53	0.11	-0.45	-0.65	-0.80
s-C_4H_9	0.74	1.43	0.55	0.14	-0.27	-0.64	b
C_6H_{11}	0.72	b	0.53	0.06	-0.37	-0.68	b
t-C_4H_9	0.77	b	0.58	b	-0.25	-0.63	b

[a]Volts vs. SCE.

[b]Not observed.

TABLE II

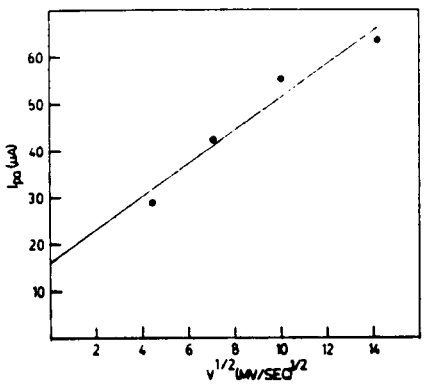
CYCLIC VOLTAMETRIC PARAMETERS OF THE Ox1/R1 COUPLE OF THE $[Rh_2(RNC)_4(dpm)_2][PF_6]_2$ COMPLEXES IN THE CH_2Cl_2/TBAH SYSTEM

R	V[a]	E_{pa} Ox1[b]	E_{pc}R1[b]	ΔE[b]	$E_{1/2}$[b]	i_{pa}[c]	i_{pc}[c]	i_{pa}/i_{pc}
n-C_4H_9	20	0.64	0.51	0.13	0.58	29	29	1.00
	50	0.65	0.49	0.16	0.57	42	42	1.00
	100	0.67	0.46	0.21	0.57	55	50	1.10
	200	0.71	0.43	0.28	0.57	64	61	1.05
i-C_3H_7	20	0.67	0.56	0.11	0.62	24	22	1.09
	50	0.68	0.54	0.14	0.61	36	34	1.06
	100	0.71	0.52	0.19	0.62	47	44	1.07
	200	0.75	0.48	0.27	0.62	57	53	1.08
s-C_4H_9	20	0.68	0.57	0.11	0.63	23	19	1.21
	50	0.70	0.54	0.16	0.62	35	31	1.13
	100	0.72	0.53	0.19	0.63	44	39	1.13
	200	0.75	0.49	0.26	0.62	56	50	1.12
C_6H_{11}	20	0.66	0.56	0.10	0.61	24	21	1.14
	50	0.68	0.54	0.14	0.61	36	32	1.13
	100	0.71	0.51	0.20	0.61	47	41	1.15
	200	0.74	0.48	0.26	0.61	58	50	1.16
t-C_4H_9	20	0.77	0.67	0.10	0.72	18	17	1.06
	50	0.81	0.65	0.16	0.73	28	25	1.12
	100	0.85	0.62	0.23	0.74	36	33	1.09
	200	0.89	0.59	0.30	0.74	44	40	1.10

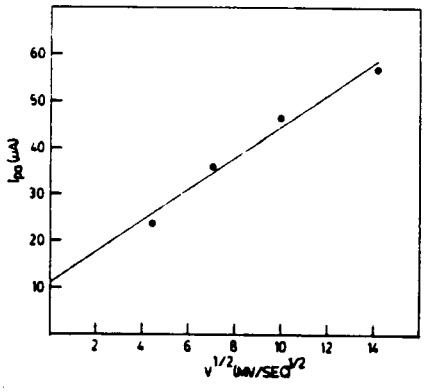
[a] Millivolts sec^{-1}.

[b] Volts vs. SCE.

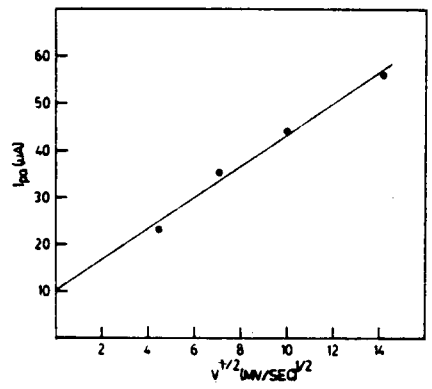
[c] Microamps.



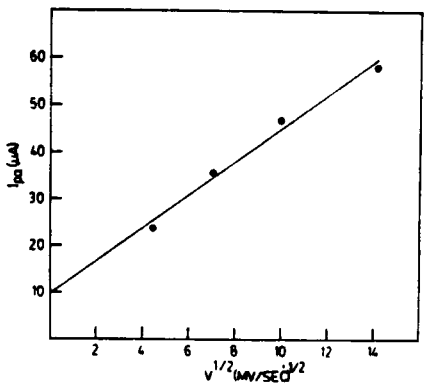
A.



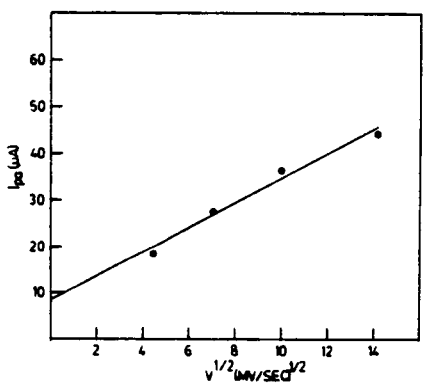
B.



C.



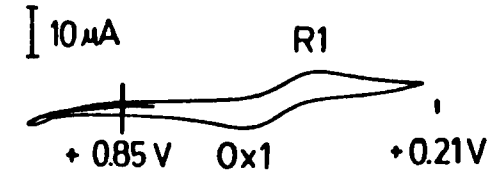
D.



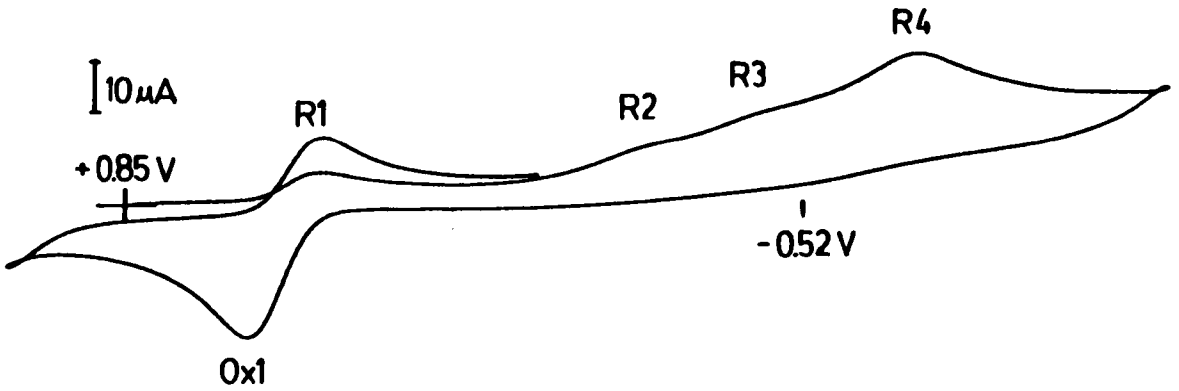
E.

Figure 4. Plots of current versus the square root of sweep rate for $[(RNC)_4Rh_2(dpm)_2][PF_6]_2$ complexes:

A. R = $\underline{n}$-C_4H_9; B. R = $\underline{i}$-C_3H_7; C. R = $\underline{s}$-C_4H_9; D. R = C_6H_{11}; E. R = $\underline{t}$-C_4H_9.



A.



B.

Figure 5. Cyclic voltammogram of $[(\underline{n}\text{-}C_4H_9NC)_4Rh_2(dpm)_2][PF_6]_2$ after oxidation at +0.85 volts in the CH_2Cl_2/TBAH system.

Conditions A and B: Conc. 1 x 10^{-3}M; 0.1M TBAH; sweep rate 100 mV sec^{-1}; SCE.

even though the initial oxidation product is not stable. Equation 7 summarizes the oxidation process.

$$[(n\text{-}C_4H_9NC)_4Rh_2(dpm)_2]^{2+} \xrightarrow[+0.850\ volt]{-e} [(\underline{n}\text{-}C_4H_9NC)_4Rh_2(dpm)_2]^{3+} \quad (7)$$

$$\downarrow CH_2Cl_2/TBAH$$

Unidentified Products

A correlation between the ease of oxidation of complexes 2a-2e (page 1) and the size of the isocyanide ligand is evident from the data in Table I (page 26). A. L. Balch[2] observed a correlation between the bulkiness of the isocyanide ligand and the wavelength of the lowest energy electronic transition for these rhodium(I) dimers. As the steric demands of the isocyanide group increases, the Rh-Rh separation increases. As the Rh-Rh distance increases, the interaction between the d_{z^2} orbitals is reduced, decreasing the energy of the HOMO and increasing the energy of the LUMO. The increase in the separation of the HOMO and LUMO with increasing size of the isocyanide ligand means that the electronic transition moves to higher energy (lower wavelength). With the HOMO at lower energy the energy required to remove an electron from the HOMO is greater and oxidation occurs at more positive potentials. Therefore, as shown in Table II (page 27) the $E_{\frac{1}{2}}$ for complexes 2a-2e varies in the order $\underline{t}\text{-}C_4H_9NC > \underline{i}\text{-}C_3H_7NC \sim \underline{s}\text{-}C_4H_9NC \sim C_6H_{11}NC > \underline{n}\text{-}C_4H_9NC$.

2. Tetrabutylammonium Tetrafluoroborate

The voltammetric behavior of complexes 2a-2e (page 1) in the CH_2Cl_2/TBAB system is similar to that of the CH_2Cl_2/TBAH system. Figure 6 shows the voltammogram of complex 2a (page 1) in the CH_2Cl_2/TBAB system. The first oxidation wave (Ox1) occurs at +0.78 volts and

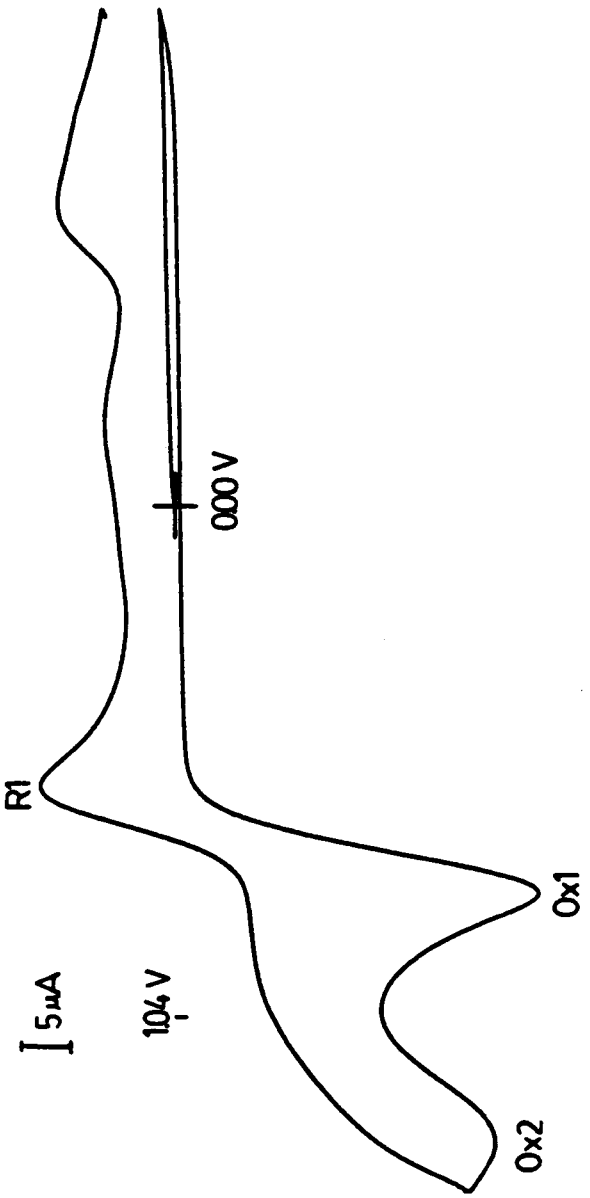


Figure 6. Cyclic voltammogram of $[(\underline{n}\text{-}C_4H_9NC)_4Rh_2(dpm)_2][PF_6]_2$ in the CH_2Cl_2/TBAB system.

Conditions: Conc. 1×10^{-3}M; 0.1M TBAB; sweep rate 100 mV sec^{-1}; SCE.

is coupled with R1 at +0.57 volts. Sweep rate studies on complexes 2a, 2c, and 2e (page 1) indicated that the Ox1/R1 couple is a quasi-reversible couple analogous to that seen with the CH_2Cl_2/TBAH system. The oxidation wave at +1.280 volts (Ox2, Figure 6) gives rise to the reduction waves near -0.15 volts and -0.59 volts.

Complexes 2b-2e (page 1) have voltammograms similar to that of complex 2a (page 1) however, the voltammogram of complex 2e differs in that the peak potential for Ox2 occurs beyond the solvent limit, Figure 7. The voltammetric peak potential data for all the complexes are presented in Table III.

Controlled potential coulometry, performed at +0.88 volts on complex 2a (page 1), indicates that Ox1 is due to an apparent one electron process (n = 1.07). The cyclic voltammogram in Figure 8 of this oxidized solution shows several reduction waves between +0.70 volts and -1.10 volts. Oxidation of complex 2a at +1.35 volts gives an electron count of 1.55. The voltammogram of the oxidized solution is shown in Figure 9. Reduction of this solution at -1.00 volts indicates a total electron transfer of 1.58 electrons per dimer. The voltammogram, Figure 10, of the solution after reduction at -1.00 volts, shows that Ox1 and Ox2 reappear. These experiments show that upon oxidation the dimeric framework is not destroyed. However, it is clear that further work is necessary to determine the nature of the products resulting from oxidation and the nature of the oxidation-reduction reactions.

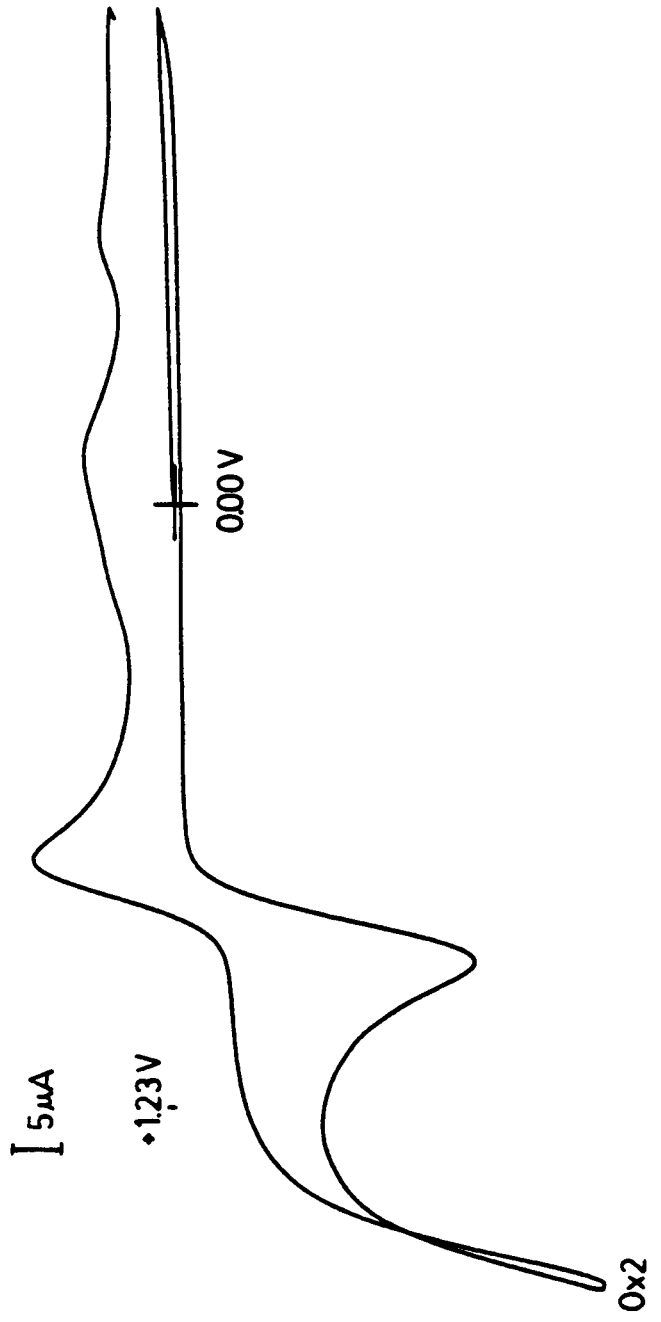


Figure 7. Cyclic Voltammogram of $[\underline{t}\text{-}C_4H_9NC)_4Rh_2(dpm)_2][PF_6]_2$ in the CH_2Cl/TBAB system.

Conditions: Conc. 1 x 10^{-3}M; 0.1M TBAB; sweep rate 100 mV sec^{-1}; SCE.

TABLE III

CYCLIC VOLTAMMETRIC PEAK POTENTIALS[a]

OF $[Rh_2(RNC)_4(dpm)_2][PF_6]_2$ COMPLEXES

IN THE CH_2Cl_2/TBAB SYSTEM

R	Ox1	Ox2	R1	R2	R3	R4	$E_{1/2}$ for Ox1/R1
n-C_4H_9	0.78	1.28	0.57	b	-0.15	-0.59	0.68
i-C_3H_7	0.81	1.30	0.56	0.04	-0.18	-0.59	0.69
s-C_4H_9	0.84	1.53	0.64	b	-0.08	-0.61	0.74
C_6H_{11}	0.82	1.52	0.61	b	-0.03	-0.63	0.72
t-C_4H_9	0.93	b	0.72	0.10	-0.08	-0.51	0.83

[a]Volts vs. SCE.

[b]Not observed.

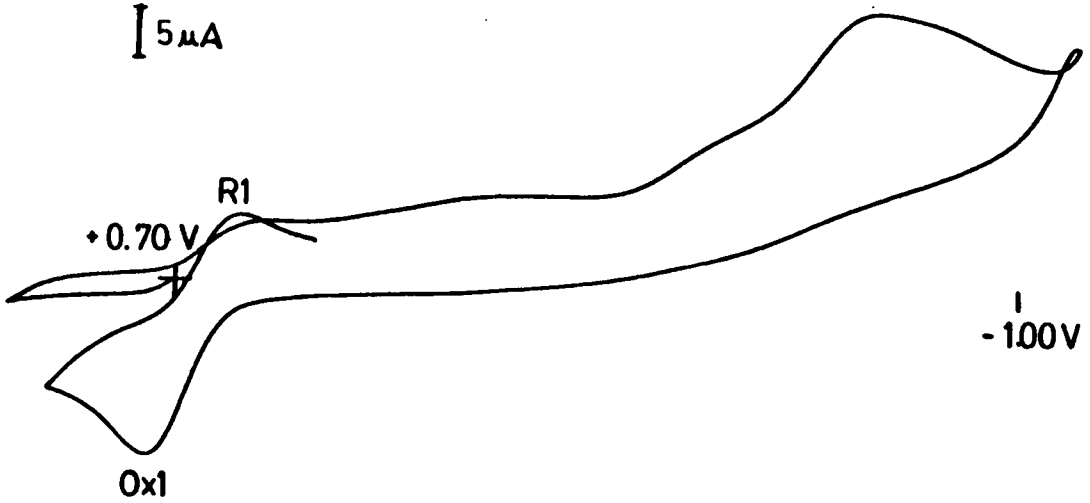


Figure 8. Cyclic voltammogram of $[(\underline{n}\text{-}C_4H_9NC)_4Rh_2(dpm)_2][PF_6]_2$ after oxidation at +0.88 volts in the CH_2Cl_2/TBAB system.

Conditions: Conc. 1 x 10^{-3}M; 0.1M TBAB; sweep rate 100 mV sec^{-1}; SCE.

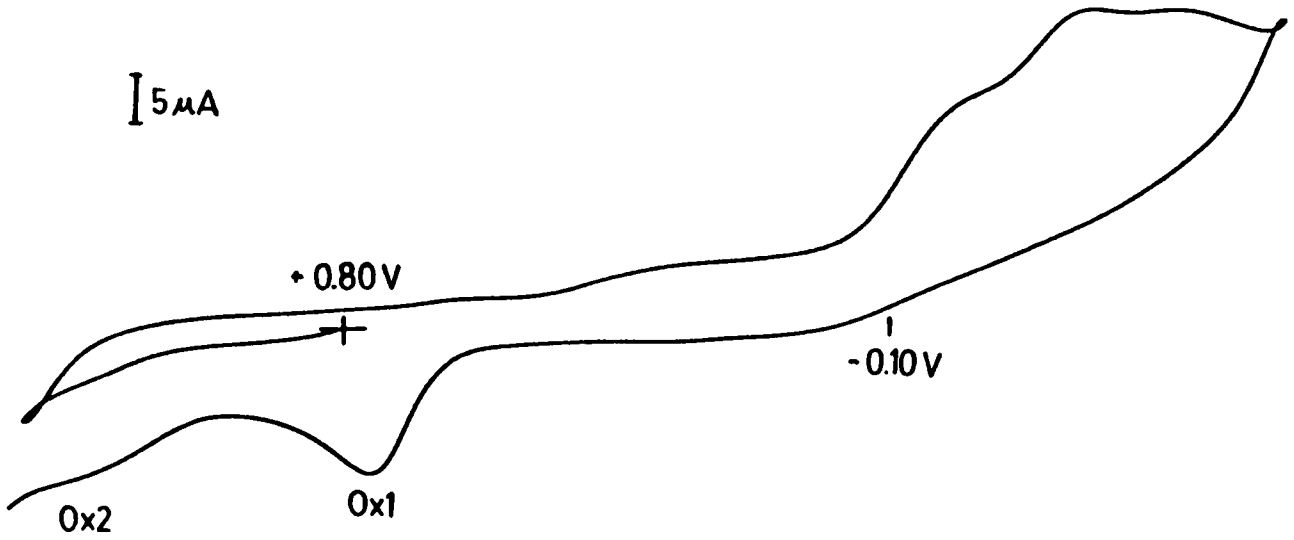


Figure 9. Cyclic voltammogram of $[(\underline{n}\text{-}C_4H_9NC)_4Rh_2(dpm)_2][PF_6]_2$ after oxidation at +1.35 volts in the CH_2Cl_2/TBAB system.

Conditions: Conc. 1 x 10^{-3}M; 0.1M TBAB; sweep rate 100 mV sec^{-1}; SCE.

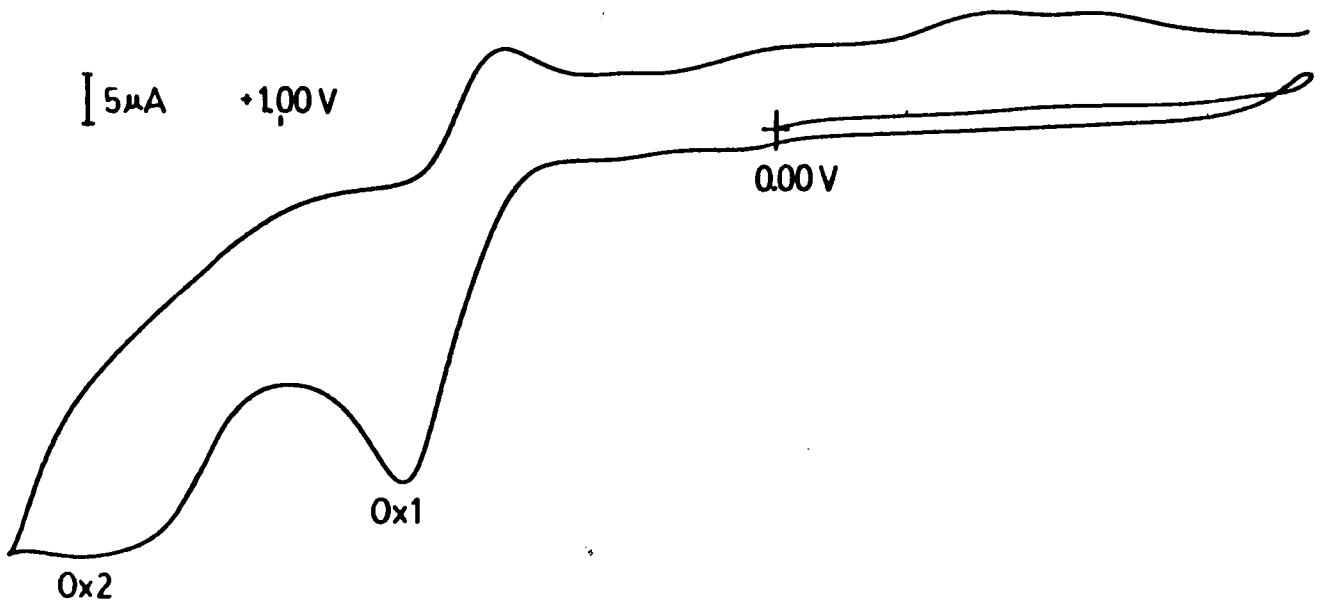


Figure 10. Cyclic voltammogram of $[(\underline{n}\text{-}C_4H_9NC)_4Rh_2(dpm)_2][PF_6]_2$ after reduction at -1.00 volts of the oxidized solution at +1.35 volts in the CH_2Cl_2/TBAB system.

Conditions: Conc. 1 x 10^{-3}M; 0.1M TBAB; sweep rate 100 mV sec^{-1}; SCE.

3. Tetrabutylammonium Perchlorate

The voltammogram of complex 2a (page 1) in CH_2Cl_2/TBAP shows two oxidation waves, one at +0.70 volts (Ox1) and one at +1.12 volts (Ox2), Figure 11A. Reduction waves R1, R2, R3, R4, and R5 appear after scanning through Ox1 and Ox2. When the potential scan in the positive direction is reversed after Ox1, the only reduction peaks which occur are R1 (+0.48 volts) and R2 (+0.21 volts), Figure 11B.

Complex 2b (page 1) in the CH_2Cl_2/TBAP system also exhibits two oxidation waves, Ox1 (+0.73 volts) and Ox2 (+1.15 volts), Figure 12A. After scanning through Ox1 and Ox2 several reduction waves appear. When the scan is reversed after Ox1, the number of reduction waves are reduced leaving only R1 (+0.48 volts), R2 (+0.35 volts), and R3 (+0.11 volts). The peak current of R1 increases significantly while that of R2 is reduced and appears only as a shoulder on R1, Figure 12B.

Complex 2c (page 1) gives two oxidation waves, Ox1 (+0.74 volts) and Ox2 (+1.21 volts), Figure 13A. A series of reduction waves which occur after scanning through Ox1 and Ox2 are also evident. The voltammetric behavior of 2c is similar to that of 2b in that reversing the scan after Ox1 but before scanning through Ox2 leaves only R1 (+0.52 volts), R2 (+0.35 volts), and R3 (+0.14 volts), Figure 13B. Furthermore, isolation of Ox1 causes the peak current of R1 to increase such that R2 is now evident only as a shoulder on R1.

Figures 14A and 14B show that complex 2d (page 1 exhibits behavior similar to that of 2a and 2c. The two oxidation waves, Ox1 and Ox2, occur at +0.72 volts and +1.28 volts respectively. The

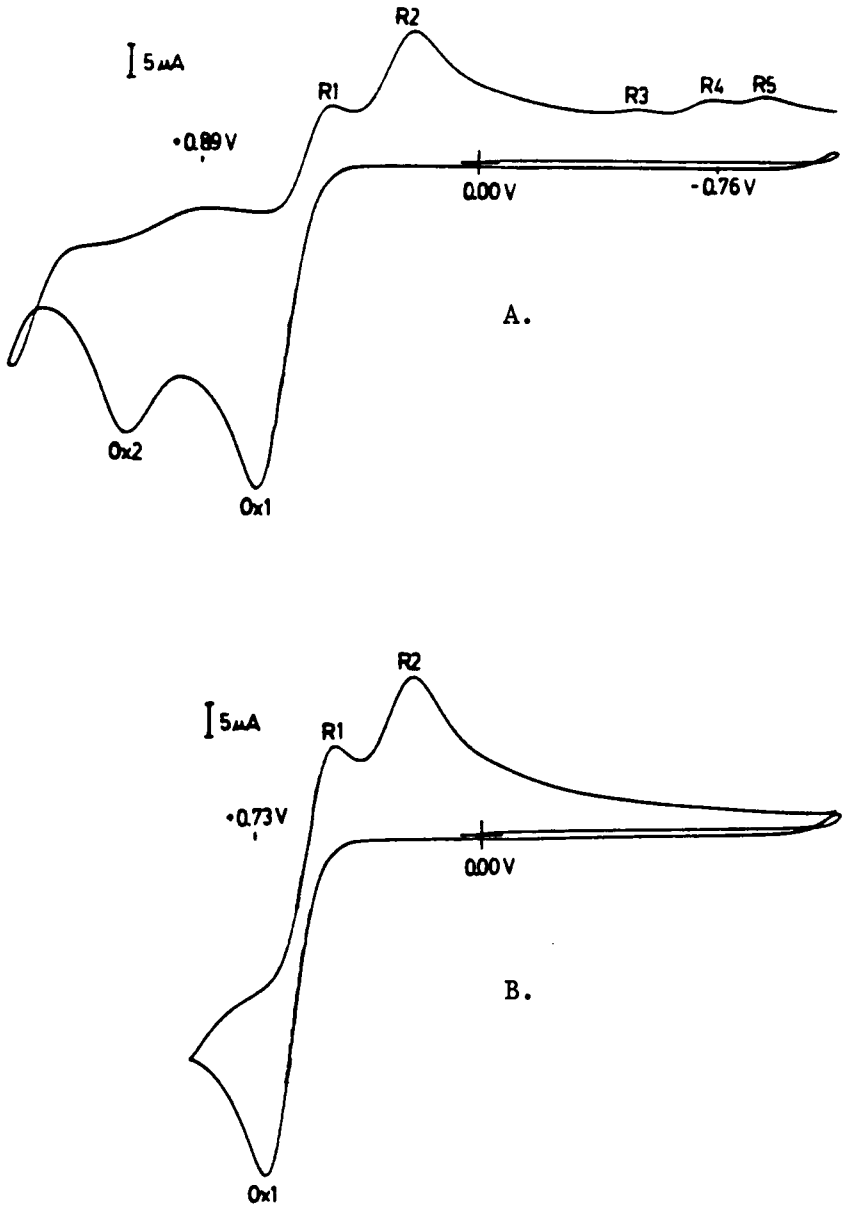


Figure 11. Cyclic voltammogram of $[(\underline{n}\text{-}C_4H_9NC)_4Rh_2(dpm)_2][PF_6]_2$ in the CH_2Cl_2/TBAP system.

Conditions: Conc. 1 x 10^{-3}M; 0.1M TBAP; sweep rate 100 mV sec^{-1}; SCE.

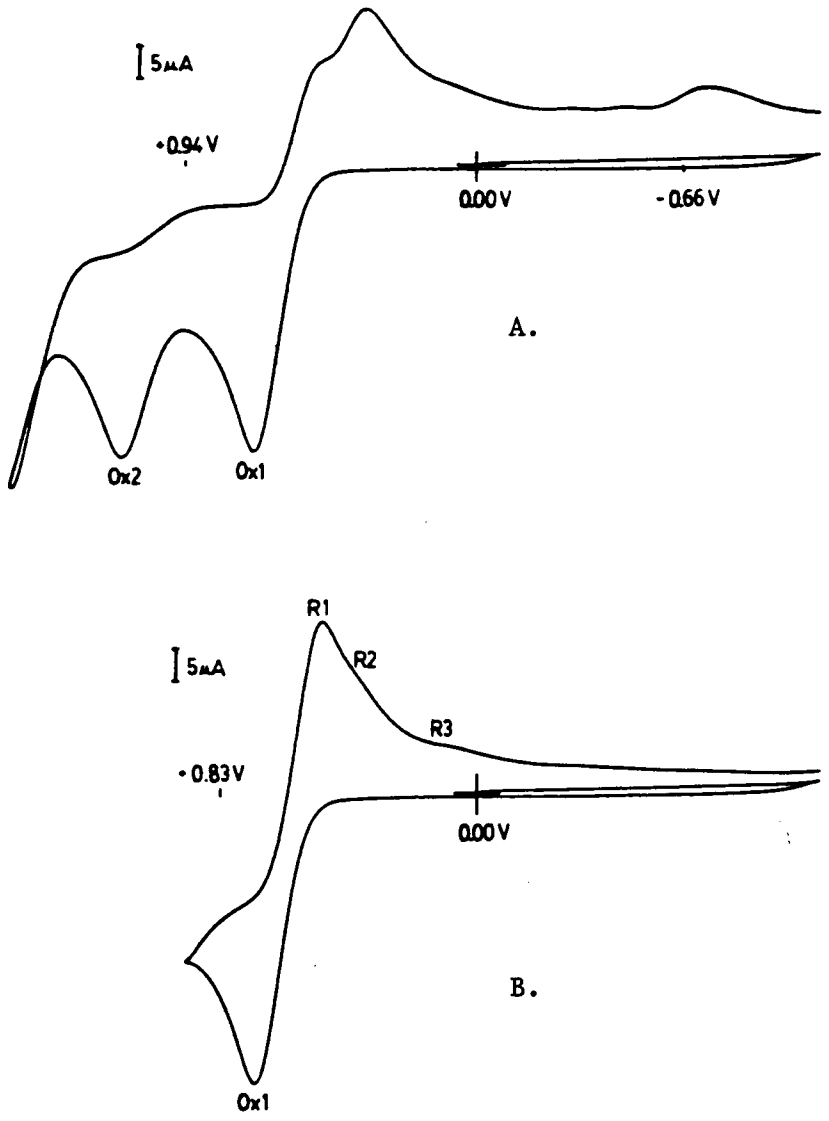


Figure 12. Cyclic voltammogram of $[(\underline{i}\text{-}C_3H_7NC)_4Rh_2(dpm)_2][PF_6]_2$ in the CH_2Cl_2/TBAP system.

Conditions: Conc. 1 x 10^{-3}M; 0.1M TBAP; sweep rate 100 mV sec^{-1}; SCE.

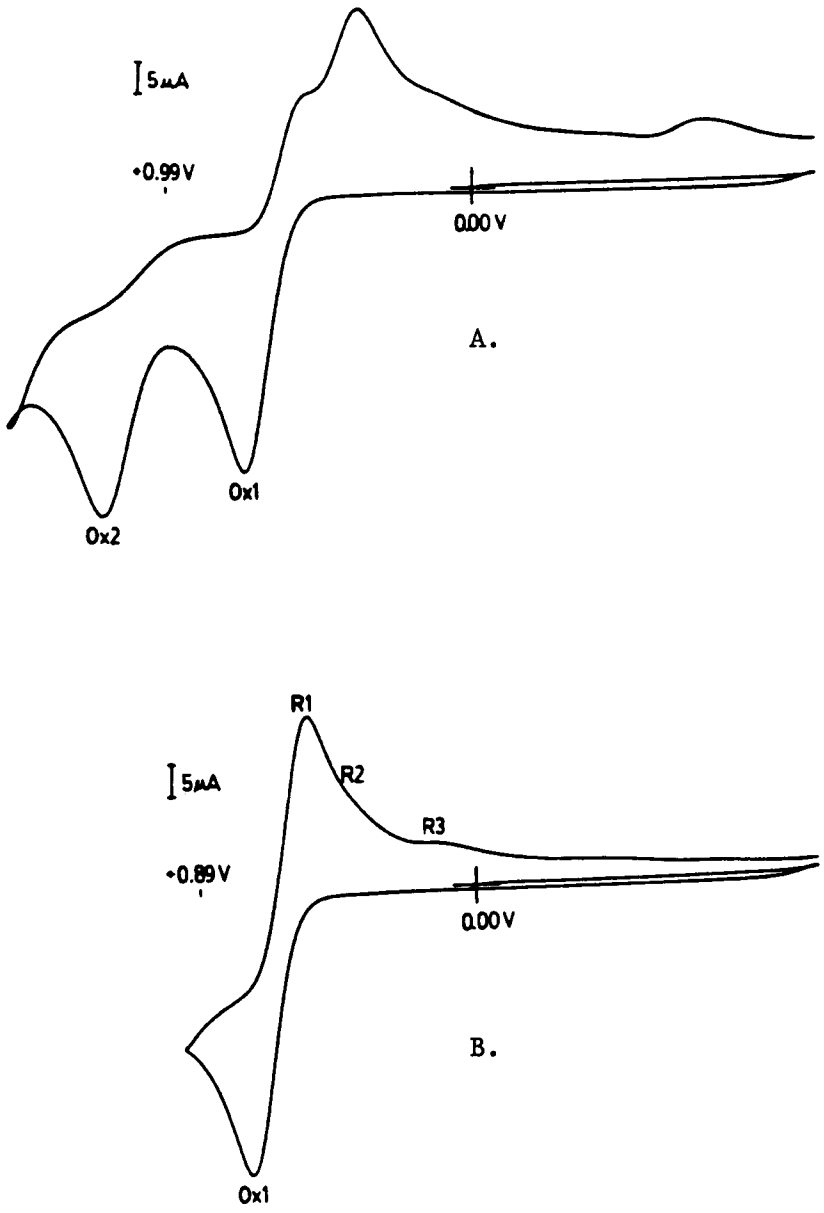


Figure 13. Cyclic voltammogram of $[(\underline{s}\text{-}C_4H_9NC)_4Rh_2(dpm)_2][PF_6]_2$ in the CH_2Cl_2/TBAP system.

Conditions: Conc. 1 x 10^{-3}M; 0.1M TBAP; sweep rate 100 mV sec^{-1}; SCE.

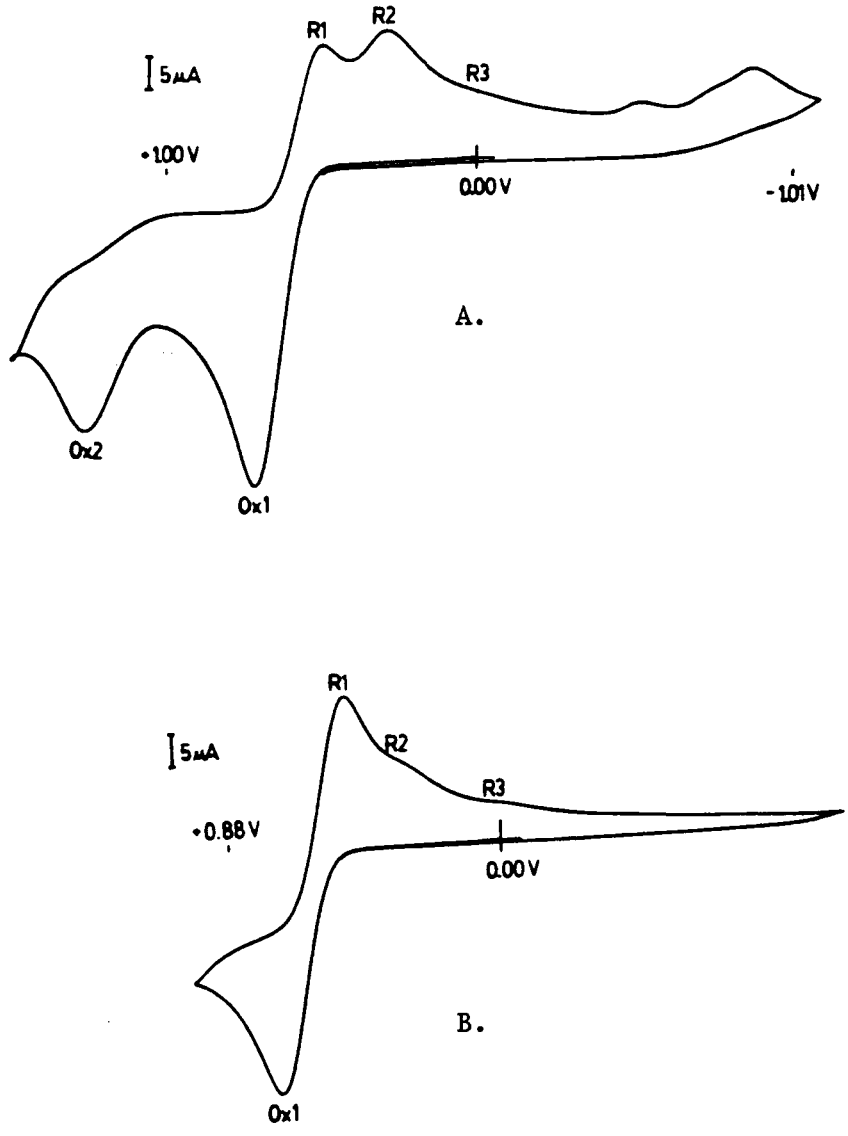


Figure 14. Cyclic voltammogram of $[(C_6H_{11}NC)_4Rh_2(dpm)_2][PF_6]_2$ in the CH_2Cl_2/TBAP system.

Conditions: Conc. 1 x 10^{-3}M; 0.1M TBAP; sweep rate 100 mV sec^{-1}; SCE.

reduction waves R1, R2, and R3 occur at +0.49 volts, +0.28 volts, and -0.01 volts respectively.

Complex 2e (page 1) shows a behavior slightly different from that of 2a, or that of 2b, 2c, and 2d. As shown in Figure 15A, 2e gives three oxidation waves Ox1, Ox2, and Ox3 at +0.83 volts, +1.14 volts, and +1.53 volts respectively. As with the other complexes, a series of reduction waves occur after sweeping to the positive limit. The results of isolation of the various oxidation waves are shown in Figures 15A, 15B, 15C. A reduction wave analogous to R2 for complexes 2a-2d is not evident, even as a shoulder, for complex 2e. R2 in Figure 15C appears to be analogous to R3 for the other complexes.

The reduction waves labeled as R2 in Figures 11-14 (pages 39 - 42) are possibly due to a follow-up reaction with, or facilitated by, the perchlorate ion. The different behaviors of the complexes appear to correlate with the size of the isocyanide groups. If R2 does represent a follow-up reaction, the reaction apparently occurs more readily for 2a (page 1) than for the other complexes and least readily for 2e (page 1).

Low temperature cyclic voltammetry was performed on complex 2a (page 1) to investigate the behavior of R2 at low temperatures. Figures 16A-16E show the voltammograms of 2a from 15°C to -49°C in the CH_2Cl_2/ TBAP system. The peak current of R2 decreases as the temperature is lowered. At -49°C R2 is no longer evident. This is consistent with a follow-up reaction since at low temperatures the reaction is expected to occur at slower rates, thereby producing less reaction product.

Previous results have suggested that the t-butylisocyanide group of complex 2e (page 1) is more sterically demanding than the other

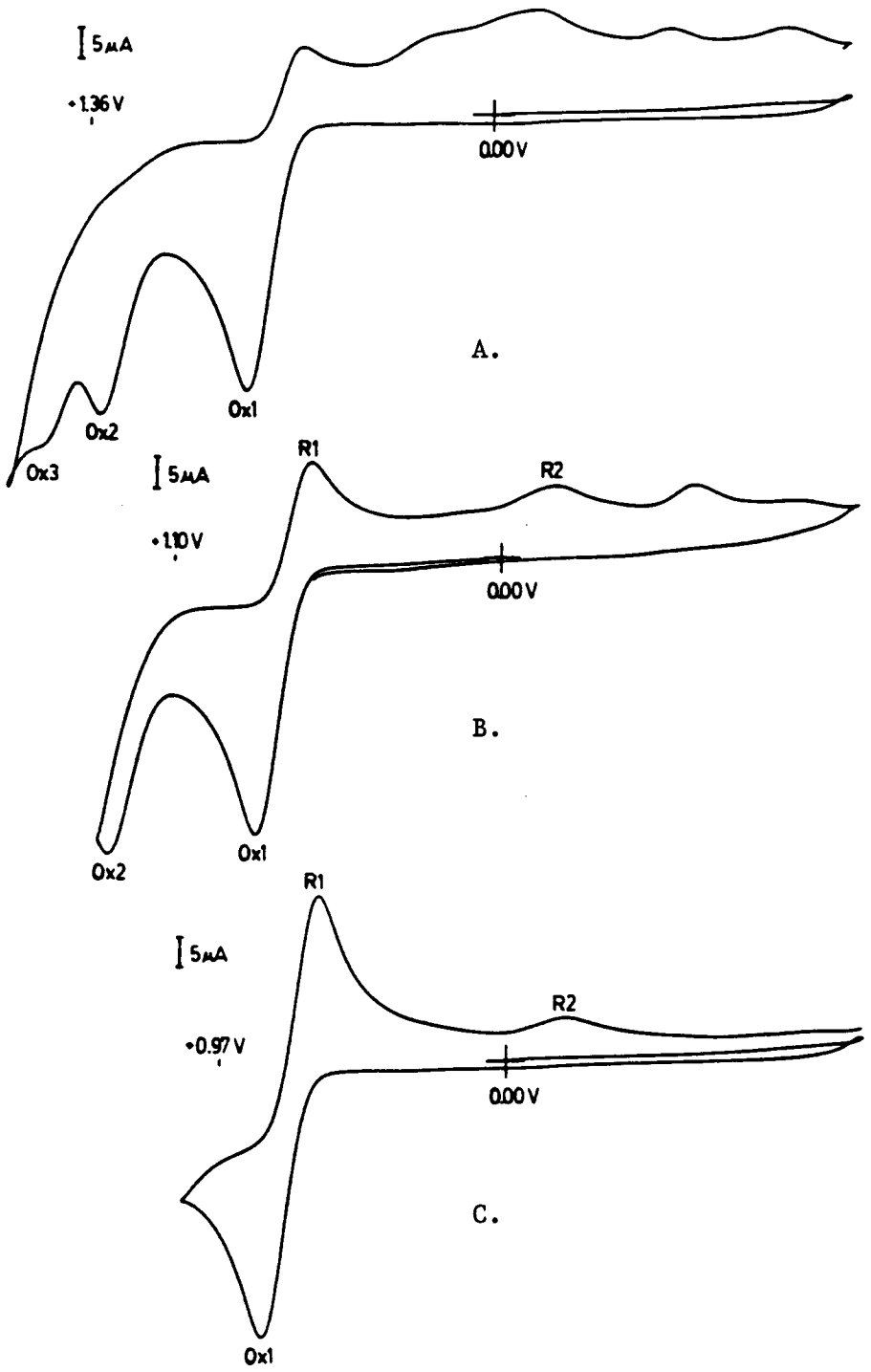
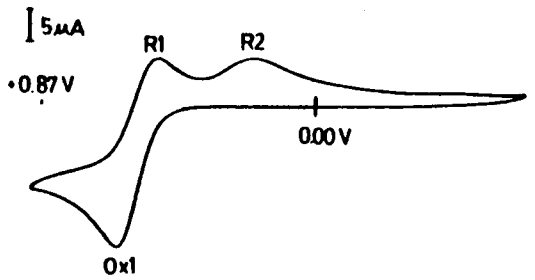
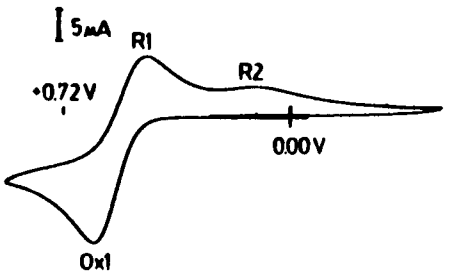


Figure 15. Cyclic voltammograms of $[(\underline{t}\text{-}C_4H_9NC)_4Rh_2(dpm)_2][PF_6]_2$ in the CH_2Cl_2/TBAP system.

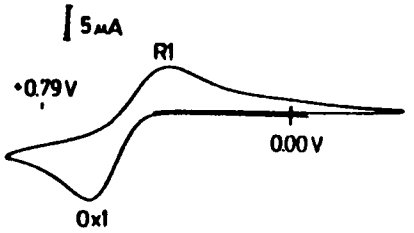
Conditions: Conc. 1 x 10^{-3}M; 0.1M TBAP; sweep rate 100 mV sec^{-1}; SCE.



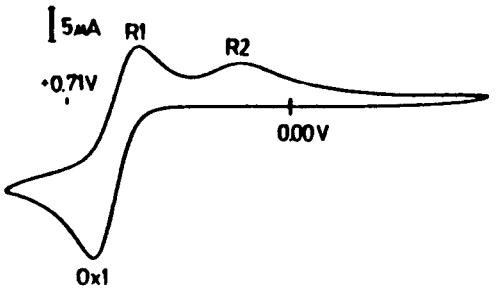
A. 15 ± 1°C



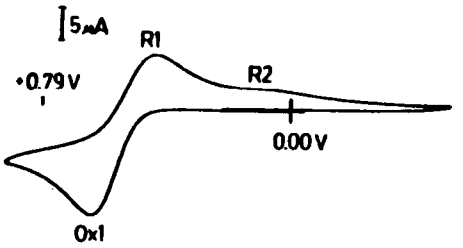
C. -22 ± 1°C



E. -49 ± 1°C



B. 1 ± 1°C



D. -36 ± 1°C

Figure 16. Low temperature cyclic voltammograms of $[(\underline{n}\text{-}C_4H_9NC)_4Rh_2(dpm)_2][PF_6]_2$ in the CH_2Cl_2/TBAP system.

Conditions: Conc. 1 x 10^{-3}M; 0.1M TBAP; sweep rate 100 mV sec^{-1}; SCE.

isocyanide ligands. Therefore, the t-butylisocyanide group should interfere with coordination of the perchlorate ion more effectively than the n-butylisocyanide, leading to a slower reaction and a smaller peak current for R2.

The electrochemical data might also be consistent with the formation of a tetrameric species similar to the tetrameric species reported for complex 1 (page 1). It seems unlikely that a tetrameric species would be stable due to steric hindrance of the isocyanide ligands and the bulky phenyl groups on the dpm. One possible formulation of such a tetrameric species is shown in Figure 17. This species is a mixed oxidation state species, Rh(I)Rh(II)Rh(II)Rh(I), which resembles the tetrameric species observed for complex 1. This structure should become less stable as the isocyanide ligand becomes more sterically demanding and is therefore consistent with the disappearance of the reduction wave near R1 as the isocyanide is changed from n-butyl to t-butylisocyanide.

Controlled potential coulometry, performed on complex 2a (page 1) past Ox1 at +0.77 volts, indicates a transfer of one electron per dimer (n = 1.0). A cyclic voltammogram of the oxidized solution shows a small wave R1 , R2 (+0.23 volts) and a new reduction wave at -0.01 volts, R3 (Figure 18). Several reduction waves near +0.80 volts are also evident. The reduction wave occurring at 0.01 volts, which does not occur on the cyclic voltammetry time scale, could be the result of a slow reaction of the oxidized complex with supporting electrolyte. It can also be seen that the redox couple, Ox1/R1, reappears after sweeping through the series of reduction waves. The $E_{1/2}$ values for the Ox1/R1 couples for complexes 2a-2e in CH_2Cl_2/TBAP are given in Table IV.

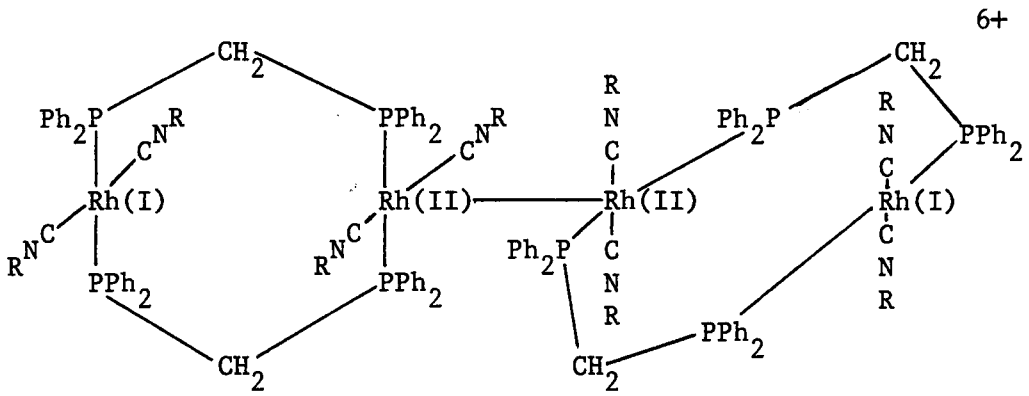


Figure 17. Possible rhodium mixed oxidation state tetrameric species.

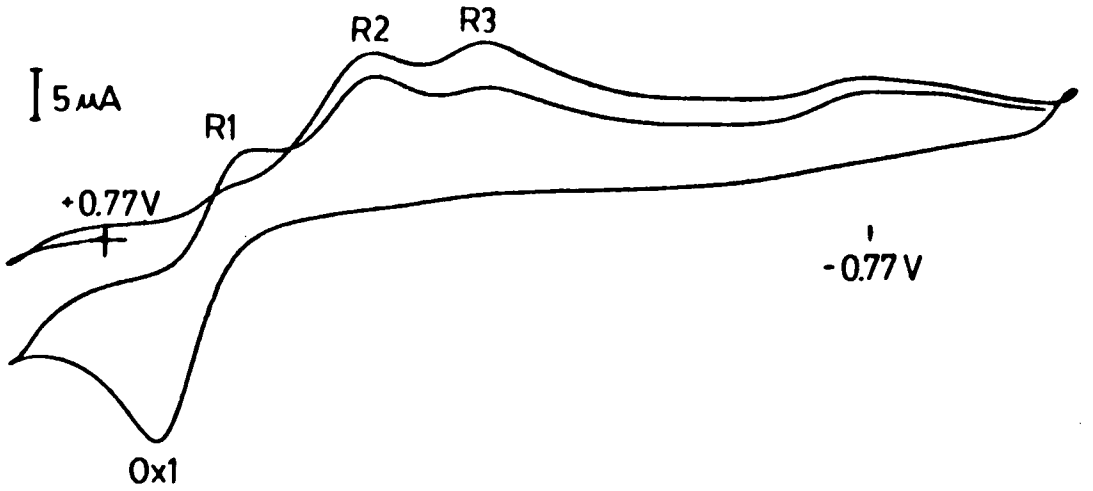


Figure 18. Cyclic voltammogram of $[(\underline{n}\text{-}C_4H_9NC)_4Rh_2(dpm)_2][PF_6]_2$ after oxidation at +0.77 volts in the CH_2Cl_2/TBAP system.

Conditions: Conc. 1 x 10^{-3}M; 0.1M TBAP; sweep rate 100 mV sec^{-1}; SCE.

TABLE IV

HALF-WAVE POTENTIALS[a] FOR $[Rh_2(RNC)_4(dpm)_2][PF_6]_2$ COMPLEXES IN THE CH_2Cl_2/TBAP SYSTEM

R	$E_{1/2}$
n-C_4Hg	0.59
i-C_3H_7	0.61
s-C_4H_9	0.63
C_6H_{11}	0.61
t-C_4H_9	0.74

[a]Volts vs. SCE

Oxidation of 2a at +1.30 volts gives an electron count of 1.8. The voltammogram of the oxidized solution is shown in Figure 19. Reduction of this solution at -0.20 volts indicates that the two reduction processes occuring at +0.21 volts and +0.06 volts, Figure 19, represents a total electron transfer of approximately one electron (n = 0.92) per dimer. Further reduction at -1.00 volts gives an additional electron count of one (n = 1.01). Figure 20 shows the voltammogram of the solution after reduction at -1.00 volts.

These experiments show that upon oxidation follow-up reactions do occur but these reactions do not destroy the dimeric framwork. Further work is necessary to determine the nature of the oxidation products and the nature of the oxidation-reduction reactions.

4. Tetrabutylammonium Nitrate

Figure 21A shows the voltammogram of complex 2a (page 1) in the CH_2Cl_2/TBAN system. This voltammogram differs from the CH_2Cl_2/TBAH and CH_2Cl_2/TBAB systems in that there is only one oxidation wave which occurs at +0.60 volts (Ox1). Ox1 is coupled with several reduction waves, the most prominent one at -0.11 volts (R1). Complex 2b (page 1) has an oxidation wave (Ox1) at +0.660 volts and three associated reduction waves at +0.02 volts (R1), -0.16 volts (R2), and -0.39 volts (R3), Figure 21B. Voltammograms of complexes 2c-2e (page 1) are similar to that of complex 2b (page 1). The peak potentials for all the complexes for the CH_2Cl_2/TBAN system are given in Table V.

Controlled potential coulometry of complex 2a (page 1) at +0.79 volts indicates an apparent electron count of two (n = 1.95). Figure 22 shows that after oxidation at +0.79 volts Ox1 disappears. However, Ox1 reappears during cyclic voltammetry if the potential scan is reversed

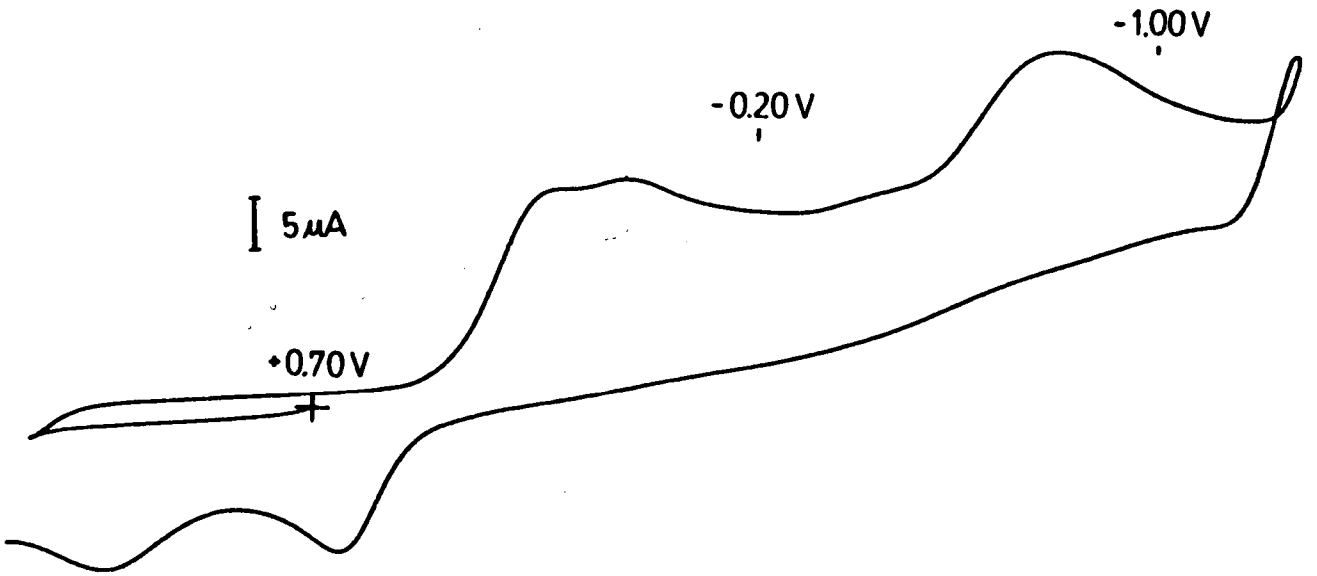


Figure 19. Cyclic voltammogram of $[\underline{n}\text{-}C_4H_9NC)_4Rh_2(dpm)_2][PF_6]_2$ after oxidation at +1.30 volts in the CH_2Cl_2/TBAP system.

Conditions: Conc. 1 x 10^{-3}M; 0.1M TBAP; sweep rate 100 mV sec^{-1}; SCE.

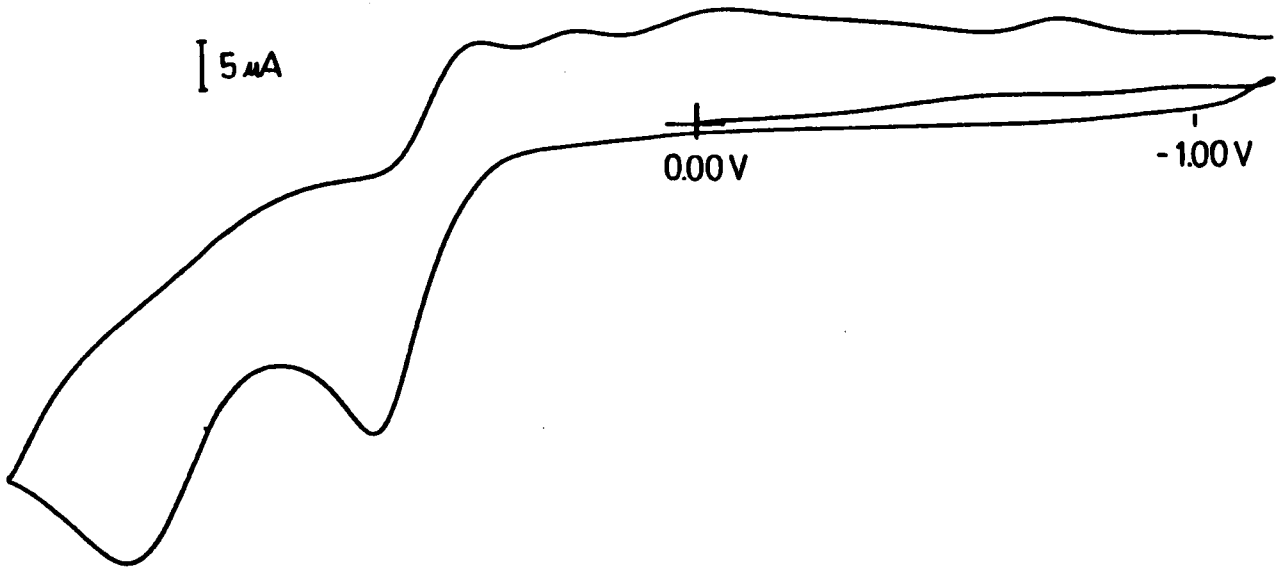


Figure 20. Cyclic voltammogram of $[(\underline{n}\text{-}C_4H_9NC)_4Rh_2(dpm)_2][PF_6]_2$ after reduction at -1.00 volts of the oxidized solution at -1.30 volts.

Conditions: Conc. 1 x 10^{-3}M; 0.1M TBAP; sweep rate 100 mV sec^{-1}; SCE.

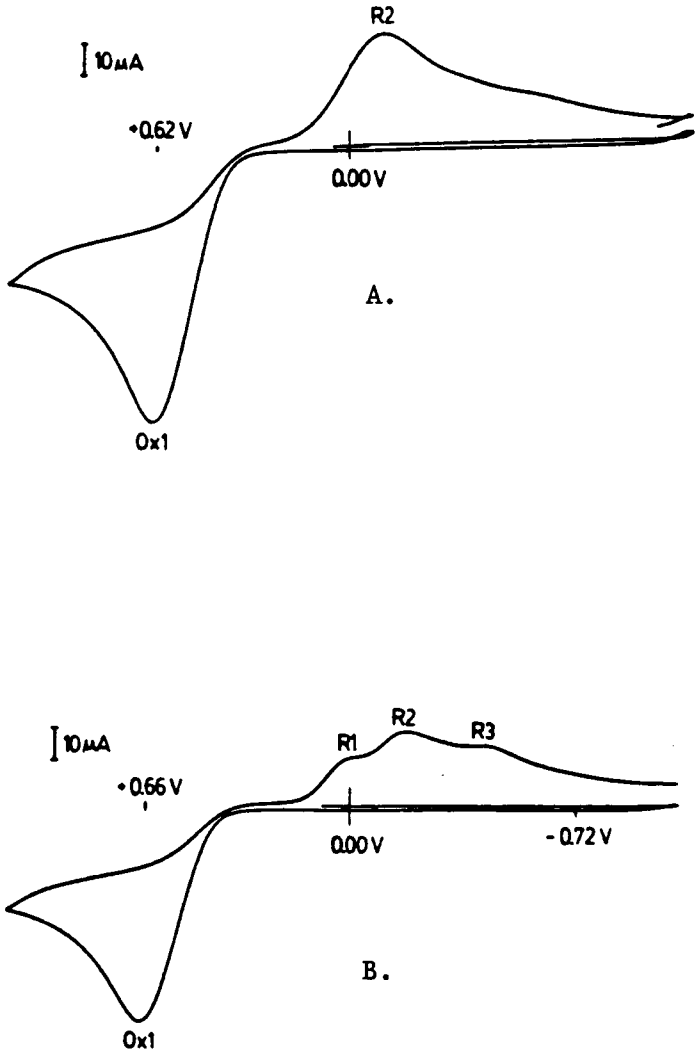


Figure 21. Cyclic voltammograms of (A) $[(\underline{n}\text{-}C_4H_9NC)_4Rh_2(dpm)][PF_6]_2$ and (B) $[\underline{i}\text{-}C_3H_7NC)_4Rh_2(dpm)_2][PF_6]_2$ in the CH_2Cl_2/TBAN system.

Conditions: Conc. 1 x 10^{-3}M; 0.1M TBAN; sweep rate 100 mV sec^{-1}; SCE.

TABLE V

VOLTAMMETRIC PEAK POTENTIALS[a] FOR

$[Rh_2(RNC)_4(dpm)_2][PF_6]_2$ COMPLEXES

IN THE CH_2Cl_2/TBAN SYSTEM

R	Ox1	R1	R2	R3
n-C_4H_9	0.60	b	-0.11	b
i-C_3H_7	0.66	0.02	-0.15	-0.39
s-C_4H_9	0.66	0.06	-0.12	-0.26
C_6H_{11}	0.66	0.00	-0.15	-0.37
t-C_4H_9	0.80	0.18	0.04	-0.16

[a]Volts vs. SCE.

[b]Not observed.

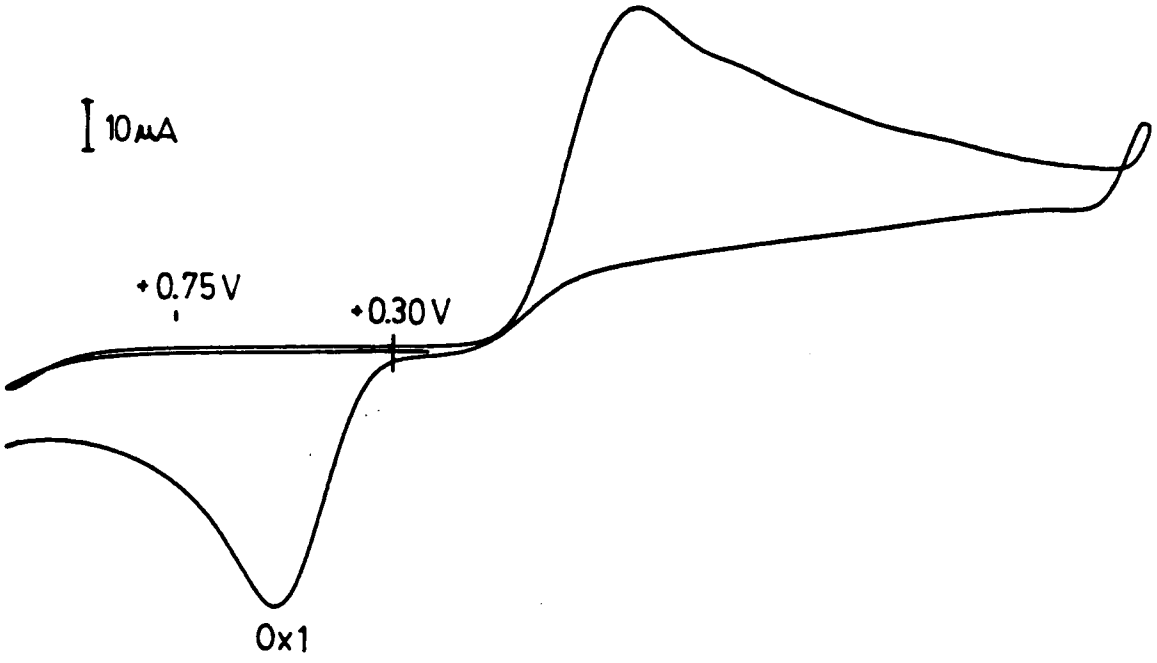


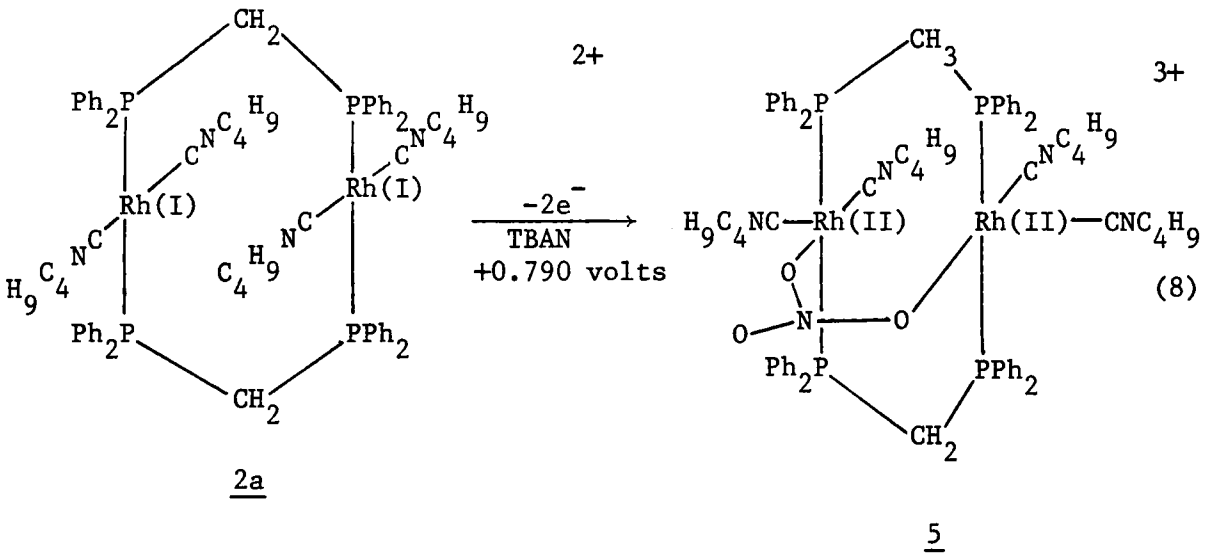
Figure 22. Cyclic voltammogram of $[(\underline{n}\text{-}C_4H_9NC)_4Rh_2(dpm)_2][PF_6]_2$ after oxidation at +0.79 volts in the CH_2Cl_2/TBAN system.

Conditions: Conc. 1 x 10^{-3}M; 0.1M TBAN; sweep rate 100 mV sec^{-1}; SCE.

at potentials more negative than the peak potentials of the reduction waves. This indicates that the original rhodium(I) dimer can be regenerated from the oxidation products.

Separation of the oxidation product from the supporting electrolyte was possible because of the high solubility of TBAN in water and the insolubility of the product in water. To eliminate the possibility of nitrate ion acting as a counter ion for the rhodium containing cation, the complex was recrystallized from methanol containing KPF_6.

The infrared spectrum of the complex shows that the isocyanide stretching frequencies shift from 2160 cm^{-1} and 2183 cm^{-1} for the parent rhodium(I) species to 2221 cm^{-1} and 2214 cm^{-1} for the oxidation product. This shift of approximately 60 cm^{-1} is indicative of a change from a rhodium(I) to a rhodium(II) species.[2] The absence of a strong broad absorption band at 1390 cm^{-1} indicates that free nitrate ions are not present.[17,18] Strong absorptions at 839 cm^{-1} and 558 cm^{-1} indicate that the hexafluorophosphate anion is present as the counter ion. The elemental analysis is consistent with the formulation, $[(\underline{n}\text{-}C_4H_9NC)_4 Rh_2(dpm)_2(NO_3)][PF_6]_3$, 5 page 20, with the nitrate being covalently bound. The IR spectrum shows that there are no bridging isocyanides. The oxidation process and the oxidation product are illustrated in equation 8.



2a

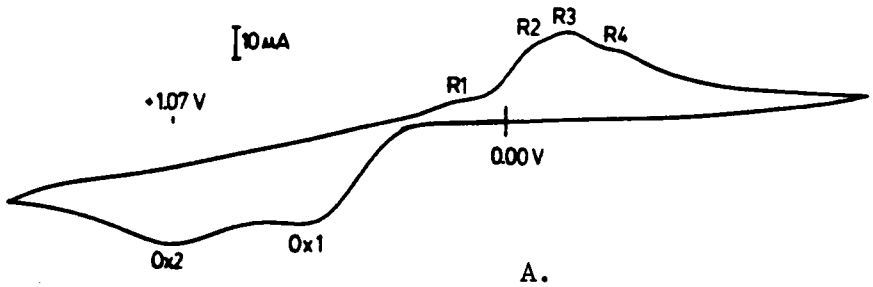
5

B. Acetonitrile

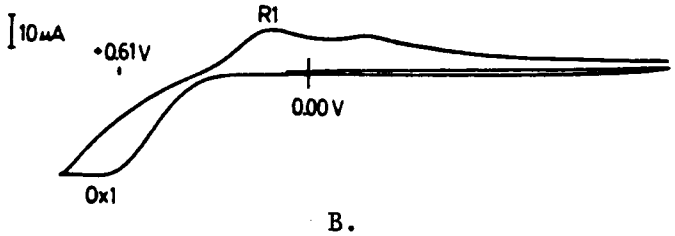
1. Tetrabutylammonium Hexafluorophosphate

Since the hexafluorophosphate anion is noncoordinating, the CH_3CN/TBAH system allows a comparison of the effects of the solvents CH_2Cl_2 and CH_3CN. The voltammogram for complex 2a (page 1) is shown in Figure 23A. The CH_3CN/TBAH system leads to two oxidation waves, Ox1 and Ox2, and associated reduction waves R1, R2, R3 and R4. When the potential scan in the positive direction is reversed after Ox1 but before Ox2, the peak current of R1 increases and the peak currents of the remaining reduction waves decrease, Figure 23B. All of the complexes have similar voltammograms and their oxidation peak potentials are in Table VI.

Because of the proximity of Ox1 and Ox2, controlled potential coulometry near the Ox1 peak potential was inconclusive and an accurate electron count for the first oxidation process (Ox1) could not be obtained. It is likely that the first oxidation process is similar to the one electron process observed using the CH_2Cl_2/TBAH system. Isolation of the



A.



B.

Figure 23. Cyclic voltammogram of $[(\underline{n}\text{-}C_4H_9NC)_4Rh_2(dpm)_2][PF_6]_2$ in the CH_3CN/TBAH system.

Conditions: Conc. 1 x 10^{-3}; 0.1M TBAH; sweep rate 100 mV sec^{-1}; SCE.

TABLE VI

VOLTAMMETRIC PEAK POTENTIALS[a] FOR COMPLEXES $[Rh_2(RNC)_4(dpm)_2][PF_6]_2$ COMPLEXES IN THE CH_3CN/TBAH SYSTEM

R	Ox1	Ox2
n-C_4H_9	0.59	1.07
i-C_3H_7	0.58	1.06
s-C_4H_9	0.56	1.05
C_6H_{11}	0.52	0.94
t-C_4H_9	0.66	1.04

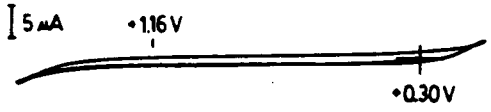
[a]Volts vs. SCE.

Ox1 wave during cyclic voltammetry of the CH_3CN/TBAH system leads to a couple analogous to the quasi-reversible one electron couple observed for the CH_2Cl_2/TBAH system except that the difference in the peak potentials of Ox1 and R1 are larger for the CH_3CN/TBAH system.

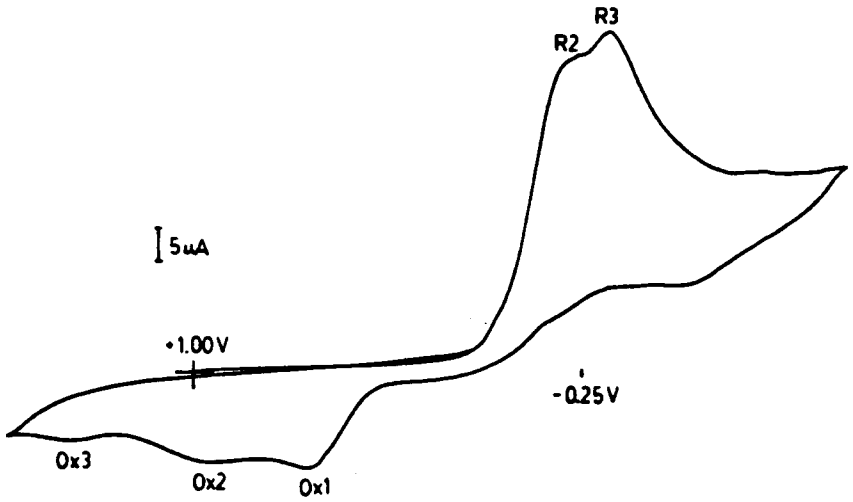
Controlled potential coulometry of complex 2b (page 1) past Ox2 at +1.300 volts indicates an apparent electron count of two (n = 1.94). Cyclic voltammograms obtained on the oxidized solutions show that the peak currents of R2 and R3 have increased. If the scan in the negative direction is reversed before the onset of R2 the waves Ox1 and Ox2 do not appear, Figure 24A and 24B. Sweeping the potential in a negative direction through the reduction waves, R2 and R3, leads to the appearance of two oxidation waves at approximately the same potentials as the original oxidation waves (Ox1, +0.68 volts; Ox2 +0.94 volts). A new oxidation wave, Ox3, occurs at +1.39 volts. Because of their very similar solubility properties, the oxidation product and the TBAH could not be readily separated.

2. Tetrabutylammonium Tetrafluoroborate

In order to avoid the complications encountered in separation of the product from the CH_3CN/TBAH system, complex 4 (page 19), the tetrafluoroborate analogue of 2b was used and TBAB was used as the supporting electrolyte. Changing the counter ion from hexafluorophosphate to tetrafluoroborate does not alter the voltammetric behavior of the complex. The moderate solubility of TBAB in water facilitates the isolation of the oxidation product.



A.



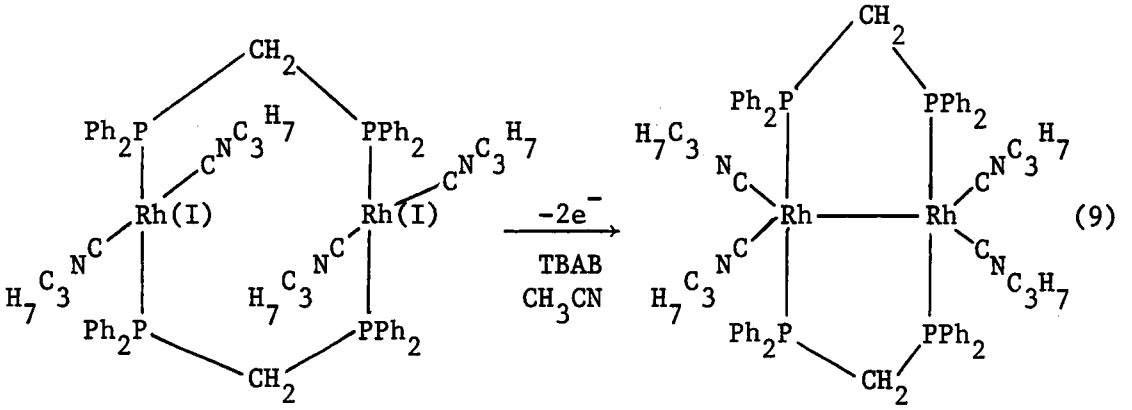
B.

Figure 24. Cyclic voltammogram of $[(\underline{i}\text{-}C_3H_7NC)_4Rh_2(dpm)_2][PF_6]_2$ after oxidation at +1.30 volts in the CH_3CN/TBAH system.

Conditions: Conc. 1 x 10^{-3}M; 0.1M TBAH; sweep rate 100 mV sec^{-1}; SCE.

Controlled potential coulomety of complex 4 (page 19) at +1.00 volt gives an apparent electron count of two (n = 1.94). The reappearance of Ox1 and Ox2 after sweeping through the reduction waves show that the dimer is not destroyed during oxidation at +1.00 volts Figure 25.

The oxidation product was separated from the supporting electrolyte by washing with copious amounts of water to remove the TBAB. The IR spectrum (KBr disk) of the product shows ν_{CN} at 2199 cm^{-1} and 2227 cm^{-1}. These frequencies are consistent with a rhodium(II) formulation.[2] Elemental analysis of the oxidation product is in agreement with the formulation $[(i\text{-}C_3H_7NC)_4Rh_2(dpm)_2][BF_4]_4{\cdot}\frac{1}{2}CH_3CN$, 6, (page 21). Equation 9 summarizes the oxidation process and gives the proposed structure of the product. The Rh-Rh bond gives an electron count of 16 for each rhodium of complex 6 (page 21).



(9)

2b 6

C. Nitromethane

1. Tetrabutylammonium Hexafluorophosphate

The voltammograms of complexes 2a-2e (page 1) in the CH_3NO_2/TBAH system appear to be quite similar to those in the CH_2Cl_2/TBAP system.

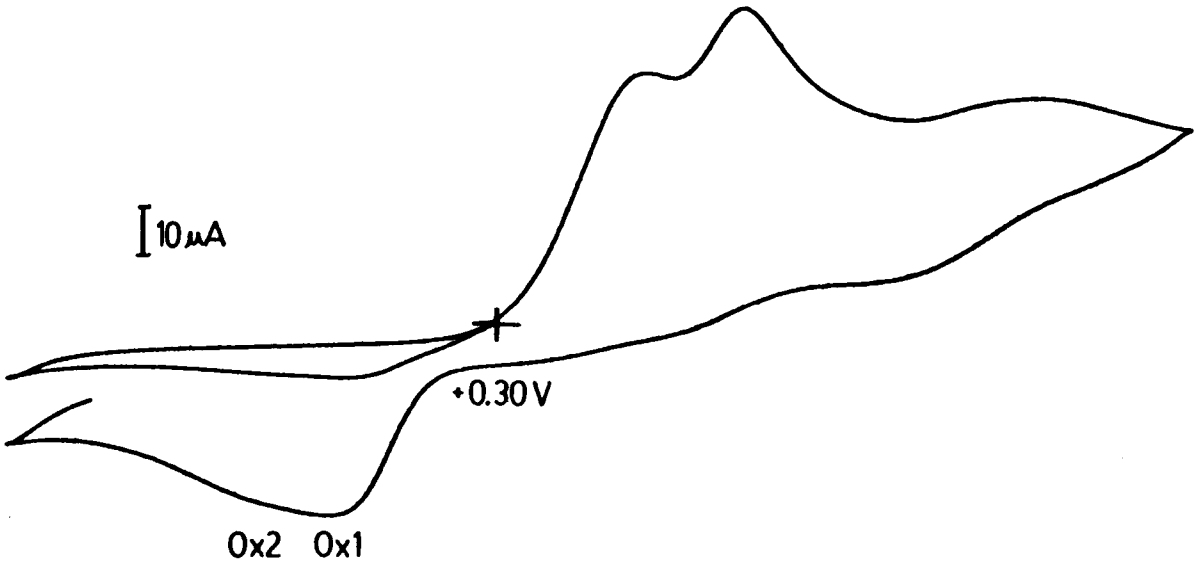


Figure 25. Cyclic voltammograms of $[(\underline{i}\text{-}C_3H_7NC)_4Rh_2(dpm)_2][BF_4]_2$ after oxidation at +1.00 volts in the CH_3CN/TBAB system.

Conditions: Conc. 1 x 10^{-3}M; 0.1M TBAB; sweep rate 100 mV sec^{-1}; SCE.

The voltammogram for complex 2b is typical of all the complexes and is shown in Figure 26A. There are two oxidation waves, Ox1 and Ox2, that give rise to several reduction waves, R1, R2, R3 and R4. Isolation of Ox1 lead to a decrease in the peak currents of R2, R3, and R4 with an increase in the peak current of R1, Figure 26B.

The Ox1/R1 couple is suggestive of an oxidative process similar to the one electron process represented by the quasi-reversible couple Ox1/R1 in the CH_2Cl_2/TBAH system, (Figure 3, page 24). In order to determine the nature of the second oxidation process (Ox2) and the role that the solvent plays, further investigations are required.

D. Summary

The investigation of rhodium(I) dimers has shown that in a non-coordinating medium such as the CH_2Cl_2/TBAH system, a quasi-reversible one electron oxidation occurs. Controlled potential coulometry has verified that the process is one electron process. Based on the MO diagram (See Figure 1, page 4), if tetramers are not formed this oxidation product should be a Rh(1½)-Rh(1½) dimer since the loss of one electron from the $1a_{2u}$ level results in an increase in the bond order of the dimer.

It has also been shown that there exists a correlation between the bulkiness of the isocyanide ligand and the ease of oxidation. The oxidation process is more facile for the least bulky isocyanide group, which is in agreement with electronic spectral data of the rhodium(I) dimers as a function of the bulkiness of the isocyanide ligand.

Studies in the CH_2Cl_2/TBAP system suggest that a follow-up reaction is occurring after oxidation; however, a number of products

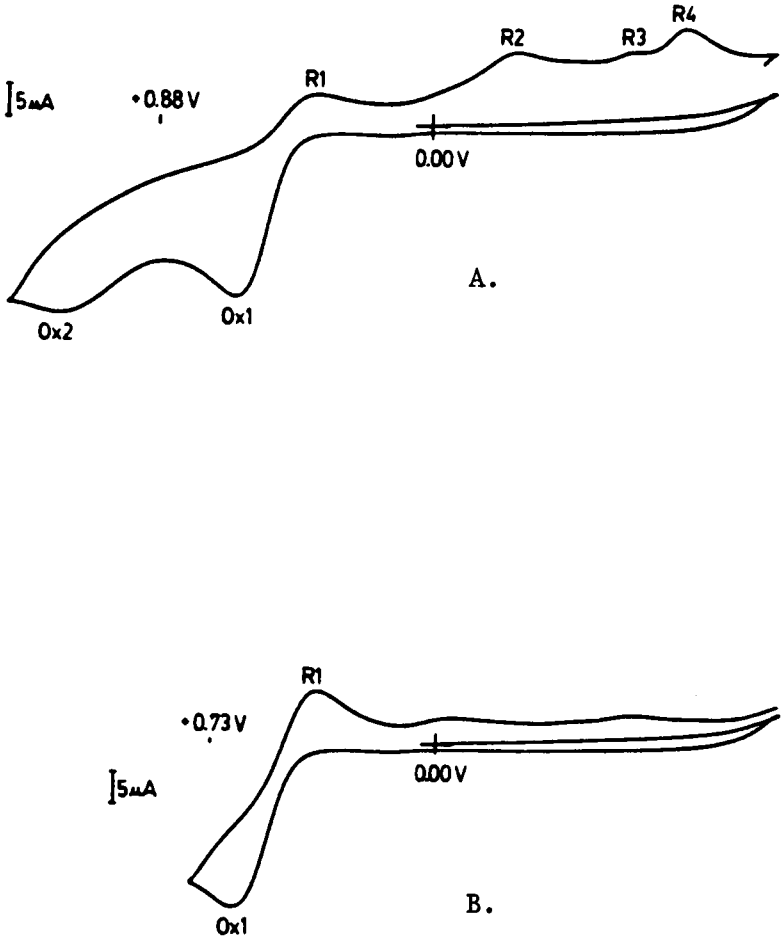


Figure 26. Cyclic voltammogram of $[(\underline{i}\text{-}C_3H_7NC)_4Rh_2(dpm)_2][PF_6]_2$ in the CH_3NO_2/TBAH system.

Conditions: Conc. 1 x 10^{-3}M; 0.1M TBAH; sweep rate 100 mV sec^{-1}; SCE.

are produced and in order to fully characterize the oxidation products of this system, additional studies are required.

Studies of the rhodium(I) dimers have shown that when more strongly coordinating species are present, the two one electron oxidation processes move toward a common potential. The peak potential of the second oxidation processes shifts closer to the peak potential of the first oxidation process until, as in the CH_2Cl_2/TBAN, only one oxidation wave is evident, leading to an apparent two electron oxidation process.

Characterization of the oxidation products of the rhodium dimers was possible for the two electron oxidation in CH_3CN/TBAH and the two electron oxidation in the CH_2Cl_2/TBAN system. In the other systems investigated, a mixture of oxidation products was obtained and could not be characterized.

The formation of the Rh(II)-R(II) species in the CH_3CN/TBAB system, complex 5 (page 57), creates possibilities of producing many new rhodium(II) dimers. In the presence of strongly coordinating anions, the Rh(II) species, complex 5 (page 57) should readily undergo addition reactions. Such studies are presently being conducted by other members of the research group.

LIST OF REFERENCES

LIST OF REFERENCES

1. N. S. Lewis, K. R. Mann, J. G. Gordon II, H. B. Gray, J. Am. Chem. Soc., 98, 7461 (1976).

2. A. L. Balch, J. Am. Chem. Soc., 98, 8049 (1976).

3. A. L. Balch, J. W. Labadie, G. Delber, Inorg. Chem., 18, 1224 (1979).

4. M. M. Olmstead, A. L. Balch, J. Am. Chem. Soc., 98, 2354 (1976).

5. K. R. Mann, J. G. Grodon II, H. B. Gray, J. Am. Chem. Soc., 97 3553 (1975).

6. K. R. Mann, N. S. Lewis, V. M. Miskowski, D. K. Erwin, G. S. Hammond, H. B. Gray, J. Am. Chem. Soc., 99, 5525 (1975).

7. V. M. Miskowski, I. S. Sigal, K. R. Mann, H. B. Gray, S. J. Milder, G. S. Hammond, P. R. Ryason, J. Am. Chem. Soc., 101, 4383 (1979).

8. I. S. Sigal, K. R. Mann, H. B. Gray, J. Am. Chem. Soc., 102, 7252 (1980).

9. K. R. Mann, B. A. Parkinson, Inorg. Chem., 20, 1921 (1981).

10. K. R. Mann, M. J. DiPierro, T. P. Gill, J. Am. Chem. Soc., 102, 3965 (1980).

11. J. Casanova, Jr., N. D. Werner, R. E. Schuster, J. Org. Chem., 31 (11), 3473 (1966).

12. J. Chatt and L. M. Venanzi, J. Chem. Soc., 4735 (1957).

13. A. J. Gordon and R. A. Ford, The Chemists' Companion; A Handbook of Practical Data, Techniques, and References (New York: John Wiley and Sons, Inc., 1972), p. 434.

14. R. P. Van Duyne and C. N. Reilly, Anal. Chem., 44 (1), 142 (1972).

15. W. S. Woodward, R. D. Rocklin, and R. W. Murray, Chem. Biomed. Environ. Instrum., 9, 95 (1979).

16. W. M. Coleman, R. K. Boggess, J. W. Hughes, L. T. Taylor, Inorg. Chem., 20, 702 (1981).

17. Addison and Logan, Advan. Inorg. Chem. Radiochem., 6 72-127 (1964).

18. F. A. Cotton and G. Wilkinson, Advanced Inorganic Chemistry, A Comprehensive Text (New York: John Wiley and Sons, Inc., 1972), p. 640.

VITA

Don Randall Womack, the second of five children, was born at Shelby Memorial Hospital, Shelby, North Carolina, on October 1, 1956. He attended Elementary School and the first year of Junior High School in Cherryville, North Carolina before moving to Hodges, South Carolina where he graduated from Greenwood High School, Greenwood South Carolina. After four years at Lander College he received a BS in Chemistry in May 1978. He then accepted a Graduate Teaching Assistantship from The University of Tennessee, Knoxville. He was awarded the MS in Chemistry from The University of Tennessee, Knoxville, in December 1981.